Spectral Analysis of Graphs by Cyclic Automorphism Subgroups*

Robert A. Davidson

Contribution No. 2780 from the Central Research and Development Department, Experimental Station, E. I. du Pont de Nemours and Company, Wilmington, Delaware 19898, USA

The theory of spectral decomposition modulo subgroups of the graph automorphism group is extended to cyclic configurations of arbitrary rotational order. By regarding graphs with cyclic automorphisms as composite polymers of relatively simple monomeric structural units, it is shown that the spectrum of eigenvalues of many prominent molecular and nonmolecular families devolves to consideration of a single monomer-derived reduction network. As the only parameter associated with this network is the set of simple circuit eigenvalues, a direct connection is forged between the spectrum of a circuit and the spectrum of any cyclic array of the same periodicity.

In addition to simplifying determination of individual graph spectra, the role of the automorphism reduction network in organizing and uniting disparate aspects of spectral theory is stressed. Systems sharing a subspectrum of identical eigenvalues are readily recognized from the graphic nature of networks. As previously, symbolic and notational devices are devised for greatest economy in the spectral analysis.
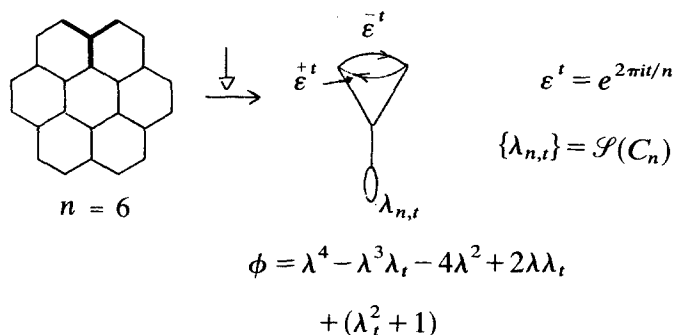
1. Introduction

This series of papers, "Unified Theory of Graph Spectral Reduction Networks," [1–3] develops a new body of methodology for the analysis and computation of graph eigenvalue spectra. The decomposition of graphs into various types of simpler networks whose spectra directly relate to the spectrum of the composite graph represents to our thinking a fundamental and obvious approach to the unraveling of complex structure-spectral relationships. We have observed that

---

* Part 4 of the series "Unified Theory of Graph Spectral Reduction Networks"

correlations of this kind are familiar in the context of molecular spectroscopy. Many examples have been put forward in developing the notion of graph families whose members share common spectral characteristics. The theme of structurally diverse graphs sharing a subset of identical eigenvalues is developed further here. It will be demonstrated that restricted consideration of π-graphs of conjugated hydrocarbons is necessarily unproductive, since analysis of this class frequently entails structures of a more general type.

The previous two contributions [2, 3] addressed the problem of graph spectral decomposition with respect to cyclic automorphism subgroups of order two. Under these groups, graphs subduce symmetric and antisymmetric reduction networks whose form is immediately evident from elementary group theoretic concepts. In many cases we were content not to call fully upon the high symmetry of a graph for spectral reduction. The resultant inefficiency is remedied now by undertaking reduction with respect to cyclic subgroups Z_n of order greater than two. Our aim is to show how graphs of arbitrary size can be regarded as *cyclopolymers* of small and fairly simple monomer generating units. Thus, all eigenvalues of coronene and the infinite family of its higher and lower congeners derive from the complex edge, four vertex, directed network and characteristic

$$\varepsilon^t = e^{2\pi it/n}$$

$$\{\lambda_{n,t}\} = \mathscr{S}(C_n)$$

$$\phi = \lambda^4 - \lambda^3 \lambda_t - 4\lambda^2 + 2\lambda\lambda_t$$
$$+ (\lambda_t^2 + 1)$$

polynomial shown above. Since the only parameter is $\lambda_{n,t}$, all cyclopolymeric structures possess spectra determined by the eigenvalues of simple circuits. This fact will permit simple, consistent derivation of exact formulas for the spectra of many prominent homologous graph series. Minor modification of cycle spectra reveals hitherto unforseen interrelations between their derivatives' spectra.

In this area of spectral graph theory as in many others, we call to the reader's attention the precocious observations of Heilbronner [4]. His insights on cyclic π-graphs are extended here to more general graphical structures. Chinese workers have recently become interested in the molecular orbital problem, also [5–7].

2. Terminology; Z_n Automorphism Reduction

The terminology and notation of graph spectral theory have been developed in earlier papers. A graph G of order p is a set $V = \{v_1, v_2, \ldots, v_p\}$ of vertices and a

set of edges $E = \{v_i v_j\}$ consisting of two-sets of vertices. A network N is a directed, loop-containing graph whose edges are weighted by complex numbers, $\omega : E \to C$. Previously, only real, arc-symmetric weights were encountered. For Z_n, $n \geq 3$ automorphism reduction certain pairs of opposite arcs bear weights which are mutually conjugate over C. The adjacency matrix of these networks exhibits hermitian symmetry, $(A^t)^*(N) = A(N)$. The spectrum $\mathscr{S}$ of a graph or network is the set of eigenvalues of its characteristic equation, $\phi(N; \lambda) = (-1)^p |A(N) - \lambda I| = 0$.

The (full) automorphism group of a graph or network, $\Gamma^0(N) = \{\gamma_i\}$, is the set of adjacency and edge-weight preserving isomorphisms of the structure, represented by permutations, $\Gamma^0 \leq S_p$. Generally, an abstract group isomorphic to $\Gamma < \Gamma^0$ is symbolized by $\mathscr{G} = \{g_i\}$. Cyclic permutation (sub)groups of S_p of order n are as usual denoted by C_n, and their abstract isomorphs by Z_n, $Z_n \cong C_n$. A Γ-orbit O_i of G or N is a maximal set of vertices equivalent by automorphisms of Γ.

It has been shown that every network or graph determines a unitary vector space $\mathscr{V}(N)$ spanned by the vertex set $V(N) = \mathscr{B}^0$. The linear adjacency operator $\hat{A}$ on $\mathscr{V}$ maps vertices of N to their neighbors according to $\hat{A} v_j = \sum_{v_i \text{ adj } v_j} \omega(e_{ij}) v_i$. The ordinary adjacency matrix $A^0 = \langle v_i | \hat{A} | v_j \rangle = \mathscr{D}^0$ is just the matrix representation of the operator $\hat{A}$ in the standard orthonormal basis. To simplify the graph eigenvalue problem, the Frobenius–Schur theory of group representations is summoned [8–11]. By well-known principles, the carrier space $\mathscr{V}(G)$ of a graph with nontrivial automorphisms admits decomposition into a direct sum of subspaces associated with the group irreducible representations (IR). The irreducible subspaces are stable under group operations and are mutually orthogonal.

A basis $\mathscr{B}$ of $\mathscr{V}$ adapted to an abelian cyclic subgroup $Z_n \leq \mathscr{G}^0$ of the graph is formulated with particular ease since the irreducible representations are one-dimensional and so coincide with the primitive characters [4, 12, 13]. If g is a generator of the cyclic group $Z_n = \{g^0 = g^n = I, g^1, g^2, \ldots, g^{n-1}\}$, the characters of Z_n in the tth irreducible representation are given by the n n^{th} roots of unity: $\{\chi_t(g^k) = e^{2\pi i k t/n} = \epsilon^{kt}\} = \{1, \epsilon^t, \epsilon^{2t}, \ldots, \epsilon^{(n-1)t}\}$.

Using the orthogonality relation we can show that the sum of cyclic group characters is nonzero only for the $t = 0$, totally symmetric, representation:

$$\sum_{k=0}^{n-1} \chi_t(g^k) = \begin{cases} n, & t = 0 \\ 0, & t \neq 0 \end{cases}.$$

The transformed basis adapted to Z_n is obtained by projecting into the tth irreducible subspace with the idempotent operator

$$\hat{P}_t : \hat{P}_t v_i = u_i = \left[\sum_{k=0}^{n-1} \chi_t(g^k) g^k \right] v_i.$$

Normalization is effected by noting that $\Gamma \cong Z_n$ orbits are either of cardinal n or cardinal 1 (for permutationally invariant vertices). The major task ahead is that of developing simple rules for the graphical expression of matrix elements $\langle u_i | \hat{A} | u_j \rangle$
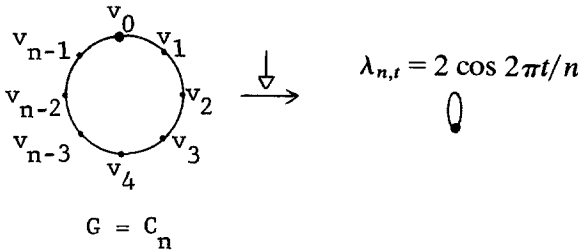
between orbit representative vertices in the new basis. We commence by examining the fundamental properties of simple circuit graphs.

2.1. Circuit Graphs, $G = C_n$

Since circuit graphs have only one orbit of cardinal n, the orthonormal basis $\mathscr{B}_t$ for the tth subspace is

$$\hat{P}_t v_0 n^{-1/2} \sum_{k=0}^{n-1} \epsilon^{kt} g^k v_0 = n^{-1/2} \sum_k \epsilon^{kt} v_k = u^{(t)}$$

and a single matrix element yields the full graph spectrum.

$G = C_n$

$$\lambda_{n,t} = \langle u^{(t)} | \hat{A} | u^{(t)} \rangle = \langle n^{-1/2} \sum_k \epsilon^{kt} v_k | \hat{A} | n^{-1/2} \sum_k \epsilon^{kt} v_k \rangle \tag{1}$$

$$= n^{-1} \langle \sum \epsilon^{kt} v_k | \sum \epsilon^{kt} (v_{k+1} + v_{k-1}) \rangle \tag{2}$$

$$= n^{-1} \langle \sum \epsilon^{kt} v_k | \sum (\epsilon^{(k-1)t} + \epsilon^{(k+1)t}) v_k \rangle \tag{3}$$

$$= n^{-1} [n(\epsilon^{-t} + \epsilon^{+t})] \tag{4}$$

$$\lambda_{n,t} = 2 \cos 2\pi t/n \qquad 0 \le t \le n-1.$$

Line (2) follows from the adjacency of v_{k+1} and v_{k-1} to v_k, line (3) simplifies subsequent evaluation of the hermitian inner product (modulo n counting is to be understood), and line (4) utilizes

$$\langle \epsilon^{jt} v_j | \epsilon^{kt} v_k \rangle = \epsilon^{-jt} \cdot \epsilon^{kt} \langle v_j | v_k \rangle = \epsilon^{(k-j)t} \delta_{jk}.$$

The reduction network is just a vertex of loop weight $\lambda_{n,t}$; when circuits occur in supergraphs, a looped vertex appears as an element of the full ARN (automorphism reduction network).

Fig. 1 presents the eigenlevel diagrams (ELD) for the leading series members. States are cyclically labeled by the IR index (t); note that (t) and $(n-t)$ pairs comprise doubly degenerate levels. Under the full group D_n the representation $\mathscr{D}^0$ reduces according to $\mathscr{D}^0 = A_1 + B_1 + E_1 + \cdots + E_{(n-2)/2}$ (n even), $\mathscr{D}^0 = A_1 + E_1 + \cdots + E_{(n-1)/2}$ (n odd). The totally symmetric A_1, $t = 0$ state with $\lambda_{n,0} = 2$ is common to all cycles, and other cosubspectral relations may be deduced from the cosine formula.
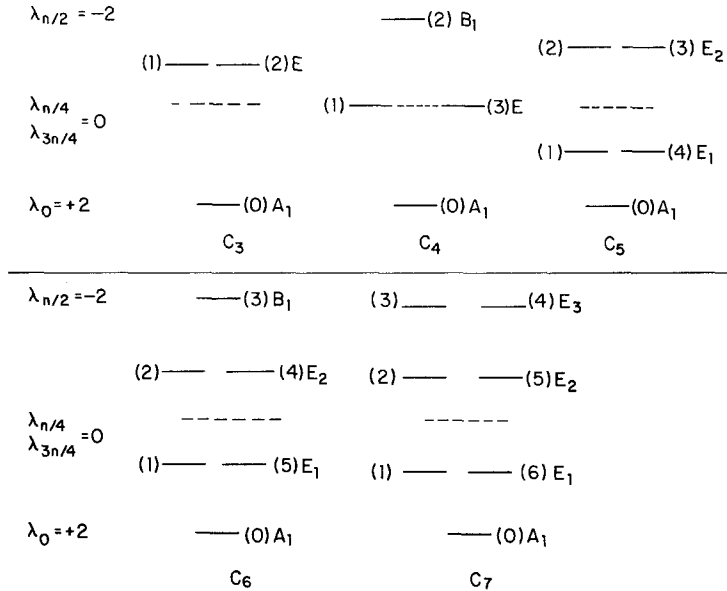
Fig. 1. ELD's of small circuit graphs

2.2. General Network Edge Weights

We proceed to consider various other types of graphical substructures and their formulation in the Γ_{Z_n}-adapted basis. Interorbit matrix elements are undertaken first.

(1) Invariant vertex orbits

Invariant vertices comprise orbits of cardinal one and appear only in the A_1 network. Suppose cyclic orbit $O_i = \{v_0^i, v_1^i, \ldots, v_{n-1}^i\}$ is adjacent to one or more of the invariant vertices. In the reduction network, edges of weight $n^{1/2}$
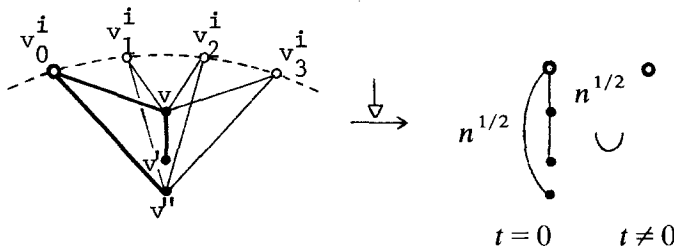
$$\langle v|\hat{A}|v\rangle = 0 \qquad \langle v|\hat{A}|v'\rangle = 1 \qquad \langle v'|\hat{A}|v''\rangle = 0 \qquad (t=0)$$

$$\langle v|\hat{A}|u_i^{(t)}\rangle = n^{-1/2}\langle v|\hat{A}| \sum \epsilon^{kt}v_k^i\rangle = n^{-1/2}\sum \epsilon^{kt}\langle v|v\rangle$$

$$= n^{-1/2}\sum \epsilon^{kt} = \begin{cases} n^{+1/2}, & t=0 \\ 0, & t\neq 0 \end{cases}$$

join a vertex representing an orbit O_i, $|O_i| = n$, to adjacent, fixed, vertices when $t = 0$. The case of $n = 2$ was examined in an earlier report [3]. While details of the $\langle u_i^{(t)} | \hat{A} | v \rangle$ calculation differ somewhat, the final result is necessarily identical. Note also that vertices which do not influence the particular interaction under consideration (e.g. other vertices adjacent to $\{v_k^i\}$) are omitted from the calculation.

(2) Adjacent orbits of order n

(a)
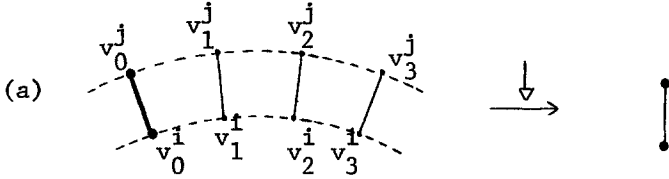
$$\langle u_i^{(t)} | \hat{A} | u_j^{(t)} \rangle = n^{-1} \langle \sum \epsilon^{kt} v_k^i | \hat{A} | \sum \epsilon^{kt} v_k^i \rangle$$

$$= n^{-1} \langle \sum \epsilon^{kt} v_k^i | \sum \epsilon^{kt} v_k^i \rangle = n^{-1} \sum \epsilon^{-kt} \epsilon^{kt} \langle v_k^i | v_k^i \rangle = 1.$$

It is assumed above that the only O_i, O_j interaction is of the sort shown, but many other possibilities present themselves.
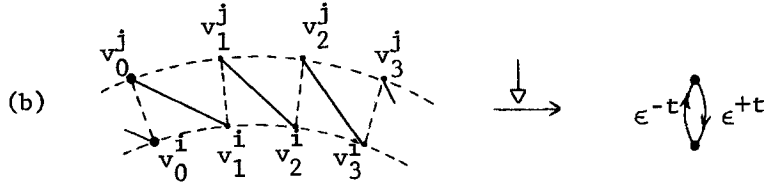
(b)

$$\langle u_i^{(t)} | \hat{A} | u_i^{(t)} \rangle = n^{-1} \langle \sum \epsilon^{kt} v_k^i | \hat{A} | \sum \epsilon^{kt} v_k^i \rangle$$

$$= n^{-1} \langle \sum \epsilon^{kt} v_k^i | \sum \epsilon^{kt} v_{k+1}^i \rangle$$

$$= n^{-1} \langle \sum \epsilon^{kt} v_k^i | \sum \epsilon^{(k-1)t} v_k^i \rangle$$

$$= n^{-1} \sum \epsilon^{-kt} \epsilon^{(k-1)t}$$

$$= \epsilon^{-t}$$

$$\langle u_j^{(t)} | \hat{A} | u_i^{(t)} \rangle = n^{-1} \langle \sum \epsilon^{kt} v_k^j | \sum \epsilon^{(k+1)t} v_k^j \rangle$$

$$= \epsilon^{+t}$$

This case supposes that a vertex v_q^i of O_i in the designated unit $\{v_q^i, v_q^j\}$ is adjacent to a vertex v_{q-1}^j of O_j in the clockwise preceding unit. If the order of connection is reversed, the directed subnetwork edge weights are transformed to their complex conjugates, i.e.

(b')
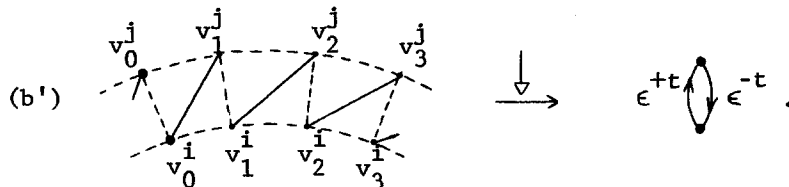
$$\langle u_i^{(t)}|\hat{A}|u_j^{(t)}\rangle = n^{-1}\langle\sum \epsilon^{kt}v_k^i|\sum \epsilon^{(k+1)t}v_k\rangle = \epsilon^{+t}.$$

Next, the combined effects of orbit interaction types (a) and (b) are explored.

(c)
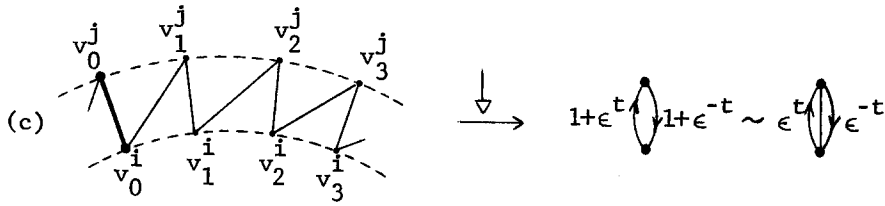
$$\langle u_i^{(t)}|\hat{A}|u_j^{(t)}\rangle = n^{-1}\langle\sum \epsilon^{kt}v_k^i|\sum \epsilon^{kt}(v_k^i + v_{k-1}^i)\rangle$$
$$= n^{-1}\langle\sum \epsilon^{kt}v_k^i|\sum (\epsilon^{kt} + \epsilon^{(k+1)t})v_k^i\rangle$$
$$= 1 + \epsilon^t.$$

Now suppose that vertices v_q^i are connected to both v_{q-1}^j and v_{q+1}^j.

(d)
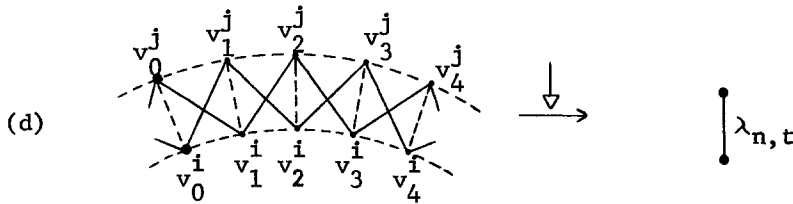
$$\langle u_i^{(t)}|\hat{A}|u_j^{(t)}\rangle = n^{-1}\langle\sum \epsilon^{kt}v_k|\sum (\epsilon^{(k-1)t} + \epsilon^{(k+1)t})v_k\rangle$$
$$= \epsilon^{-t} + \epsilon^{+t} = \lambda_{n,t}.$$

When vertices v_q^i are adjacent to v_{q+x}^j in more remote monomer units, the matrix elements are calculated in an entirely analogous fashion.

(e)
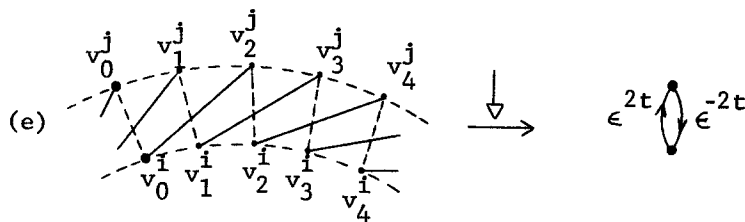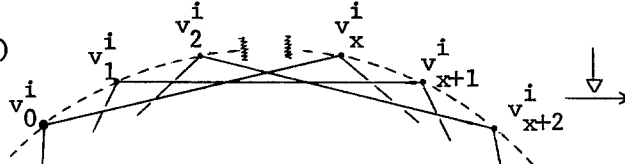
$$\langle u_i^{(t)}|\hat{A}|u_j^{(t)}\rangle = n^{-1}\langle\sum \epsilon^{kt}v_k|\sum \epsilon^{(k+2)t}v_k\rangle = \epsilon^{2t}.$$

Obviously, many combinations of these fundamental interaction types will occur in arbitrary graphs.

(3) Intraorbit calculation
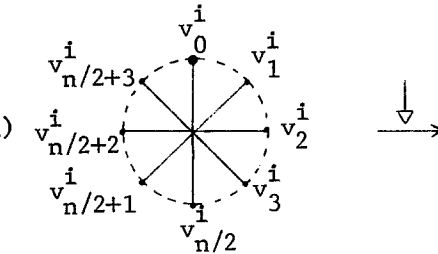
A circuit subgraph of cyclically equivalent vertices reduces to a looped vertex of weight $\lambda_{n,t}$. If the adjacent, equivalent vertices reside in monomers removed by x units, the loop weight is determined as follows.

(f)

$$\langle u_i^{(t)} | \hat{A} | u_i^{(t)} \rangle = n^{-1} \langle \sum \epsilon^{kt} v_k^i | \sum (\epsilon^{(k+x)t} + \epsilon^{(k-x)t}) v_k^i \rangle$$

$$= \epsilon^{xt} + \epsilon^{-xt} = 2 \cos 2\pi xt/n = \lambda_{n,xt}$$

Implicit in the above is that edges $e_{k,k-x}$ and $e_{k,k+x}$ are distinct. Special attention is accorded the degenerate situation when these edges are identical.

(g)

$$\langle u_i^{(t)} | \hat{A} | u_i^{(t)} \rangle = n^{-1} \langle \sum \epsilon^{kt} v_k^i | \hat{A} | \sum \epsilon^{kt} v_k^i \rangle$$

$$= n^{-1} \langle \sum \epsilon^{kt} v_k^i | \sum \epsilon^{kt} v_{k-(n/2)}^i \rangle$$

$$= n^{-1} \langle \sum \epsilon^{kt} v_k^i | \sum \epsilon^{(k+n/2)t} v_k^i \rangle$$

$$= \epsilon^{nt/2} = (-1)^t$$

Evidently, a loop of weight $(-1)^t$ is associated with this structural feature. It remains for us to demonstrate how these individual elements combine and interact to afford the reduction networks of full graphs.

2.3. Applications to Cyclopolymeric Graphs

Graphs with cyclic automorphism subgroups may be regarded for purposes of spectral analysis as polymers of fundamental monomeric building units. The repeat subgraph ("unit cell", "motif") is assembled into cyclically periodic arrays which we call *cyclopolymers*, or *cyclomers*. It is the structure of the monomer and the mode of its connection to succeeding units which will determine the spectrum of the total array. This conception can greatly simplify many large and complex graph eigenvalue problems, and establish insights at a fundamental level into the spectral affinity of graphs otherwise viewed in isolation. The component reductions of the foregoing section are now concatenated into complete reduction networks of graphs. Various aspects of the reduction process are surveyed prior to a more detailed study of selected structures.

We first observe that graphs of certain forms may be representative of general classes of structures (homologous families) whose members are related by defined

rules of elaboration. When symmetry or structural singularities are absent from such a series, it is obviously advantageous to formulate the reduction network, its characteristic polynomial and possibly the spectrum itself in the most general terms. As an example let us obtain the spectrum of the pyramid or wheel graph, $W_n = C_n + K_1$. There is in fact nothing essential remaining to compute or reason over, since the wheel structure and our development of cyclic group representations allows us to write $N(W_n)$ by inspection. A point is taken from each Γ_{Z_n}

$$W_5 \qquad W_6 \qquad N(W_n) \qquad A_1 \ (t=0) \qquad t \neq 0$$

$$\mathcal{G}^\circ : \underline{D}_5 \qquad \mathcal{G}^\circ : \underline{D}_6$$

$$\phi(N_{A_1}) = \lambda^2 - 2\lambda - n$$

$$\mathcal{S}(N_{A_1}) : \{1 \pm (n+1)^{1/2}\}$$
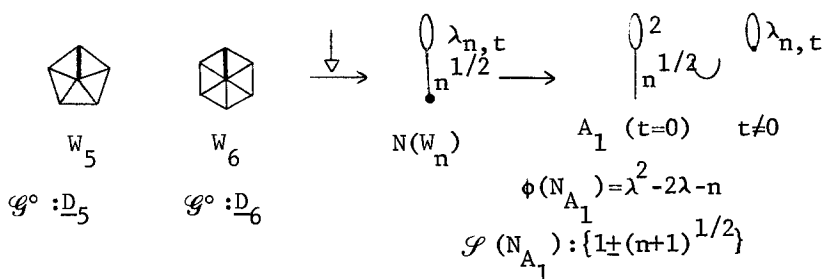
orbit to form the basic monomer subgraph, whose adjacency with following units is scrutinized. In this case the circuit reduces to a looped vertex of weight $\lambda_{n,t}$, which is joined to the fixed vertex in the $t = 0$ IR by an edge of weight $n^{1/2}$. The distinction between $t = 0$ and $t \neq 0$ is made explicit above, and this affords a simple expression for all wheel eigenvalues [14, 15]. All but two of these are roots of the peripheral cycle, which explains our unconventional definition of the graph. In similar fashion the spectrum of a bipyramidal graph $C_n + 2K_1 = C_n + \bar{K}_2$ is $\{1 \pm (2n+1)^{1/2}, 0, \lambda_{n,t\neq0}\}$. A homologous series in the invariant vertices is also suggested. The reduction network immediately tells us that members of the latter family with fixed n are cosubspectral in the circuit eigenvalues.

The family of graphs consisting of an n-ring surrounded by n ortho-fused 6-rings to which the prominent molecule coronene belongs was noted in the introduction. See Fig. 2. The repetition motif of a cyclomer generally admits of a multiplicity of representations, all of which are, however, cospectral. To avoid needless complication our monomer subgraphs will always be connected. Even then, Fig. 2 illustrates that several forms present themselves; any one of maximal symmetry (*vide infra*) may be utilized. *The cospectral reduction networks N and N' are abbreviated to show only the ϵ^{+t} directed edge.* Since hermitian matrices A and their adjoints A^{*t} are cospectral, the direction of the edge weighted ϵ^t is arbitrary when only one such edge occurs. The general dinetwork N of Fig. 2 is asymmetric, but in the A_1 representation pairs of conjugate directed edges collapse to a symmetric edge of weight one (e.g. (d)). The resultant symmetry enhancement occasions further automorphism reduction.

Let us correlate the reduction of coronene-type graphs under the full D_n group and under its normal subgroup C_n. For even n the D_n IR multiplicities are $(3A_1 + A_2) + (3B_1 + B_2) + 4 \sum_{i=1}^{(n-2)/2} E_i$, and for odd n, $(3A_1 + A_2) + 4 \sum_{i=1}^{(n-1)/2} E_i$. By explicit calculation or the network order of four in Fig. 2 it is clear that single reduction by a cyclic subgroup is less complete than by the full automorphism
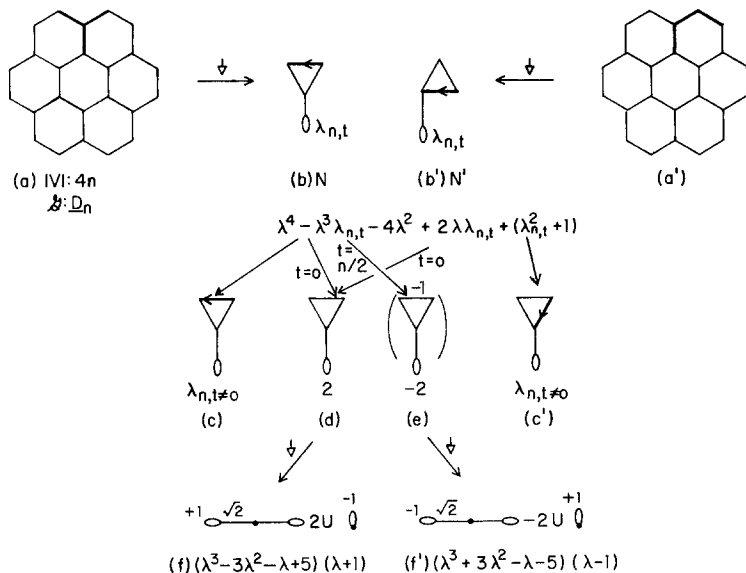
Fig. 2. Reduction of coronene-like graphs

group. It has been noted, however, that the A_1 network (d) from C_n has a symmetry axis and further reduction (f) yields the result predicted from its D_n supergroup. Likewise, when n is even the IR $t = n/2$ yields a symmetric, negative edge network (e) whose reduction is again in conformity with D_n expectations. It has been shown previously [2] that (f) and (f') are of necessity antispectral. It is expected generally that the nondegenerate $t = 0$ and $t = n/2$ levels of even circuits will correlate with cyclopolymer subspectra which are potentially reducible. All even coronene-family members therefore contain a subspectrum of eight common eigenvalues, and all share the A_1 subspectrum. Other spectral relations follow from the nature of the circuit eigenvalues.

From the $t = 0$, $n/2$ arc-symmetric networks we can easily account for cosubspectral graphs which have no obvious structural similarity. Surprising and fascinating coreductions are plentiful; the A_1 coronene-family network, for example, is also associated with the class of graphs shown below. Observe that full factorability is evident only from the N network of Fig. 2, not from its cospectramer N'.
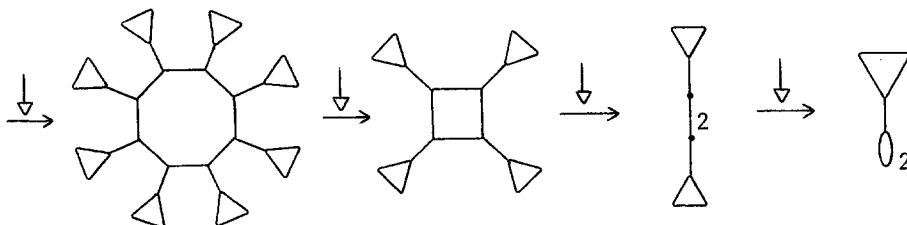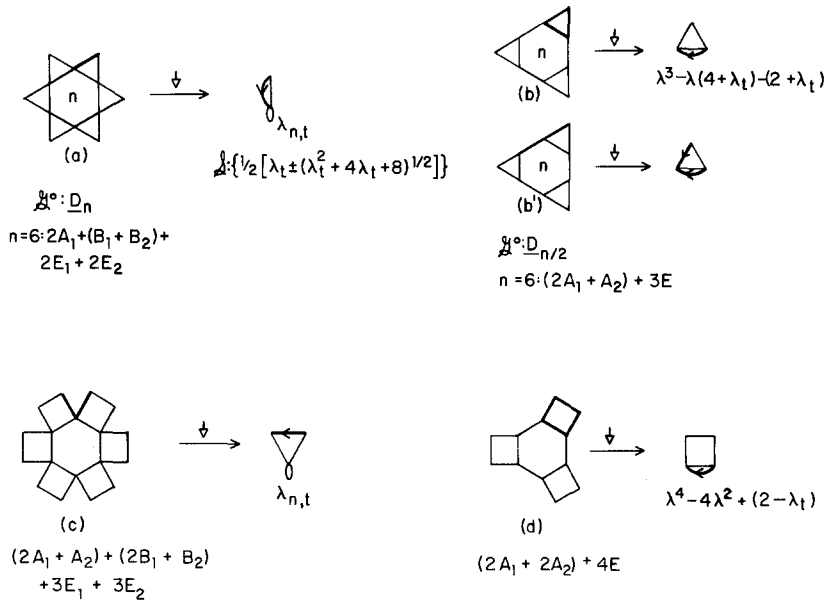
Fig. 3. Irreducible representation multiplicity for two pairs of graphs

The question arises whether Z_n reduction will always *ultimately* provide the same degree of factorization as its higher precursors in the group lattice. We are inclined to believe that it will, though there may be exceptions in highly symmetric, e.g. transitive, graphs. It is just in these difficult situations, however, that the power and simplicity of our methods are fully realized.

Fig. 3 investigates the reduction of two structurally similar pairs of graphs, (a), (b) and (c), (d). Under D_m all these graphs feature two orbits, and it might be suspected that second order networks result from all of them. This is neither confirmed by group theory nor evidenced by the reduction networks. We have nevertheless been intrigued by the possibility that the special conjugate weight relation of converse dinetwork edges could be utilized for "hermitian symmetric" and "hermitian antisymmetric" factoring of, for example, cyclic networks of the

following kind. At present we have no justification for such supersymmetry factoring. Reduction can be effected, however, on the basis of the bipartite character of even cycles, as we now discuss.

Binetworks with complex edge weights are represented by hermitian adjacency matrices of the block structure shown.

$$A = \begin{pmatrix} 0 & P_{bxw} \\ P_{wxb}^{*t} & 0 \end{pmatrix} \qquad A^2 = \begin{pmatrix} (PP^{*t})_b & 0 \\ 0 & (P^{*t}P)_w \end{pmatrix}$$

$$\mathscr{S}(A) = \{\lambda_i\} \qquad\qquad \mathscr{S}(A^2) = [\mathscr{S}(A)]^2 = \{\Lambda_i\}$$

The bipartite reduction network with squared eigenvalues $\Lambda_i = \lambda_i^2$ is formed in the same manner as for graphs, the difference being that network loop weights for vertices incident with complex weighted arcs entail the product of conjugate arc weights rather than their square [1]. Fig. 4 compares the bipartite reduction of the o-, m-, and p-cyclopolyphenylenes. For the ortho and para cases, it is shown that Z_n reduction followed by bipartite reduction of the ARN yields the same result as
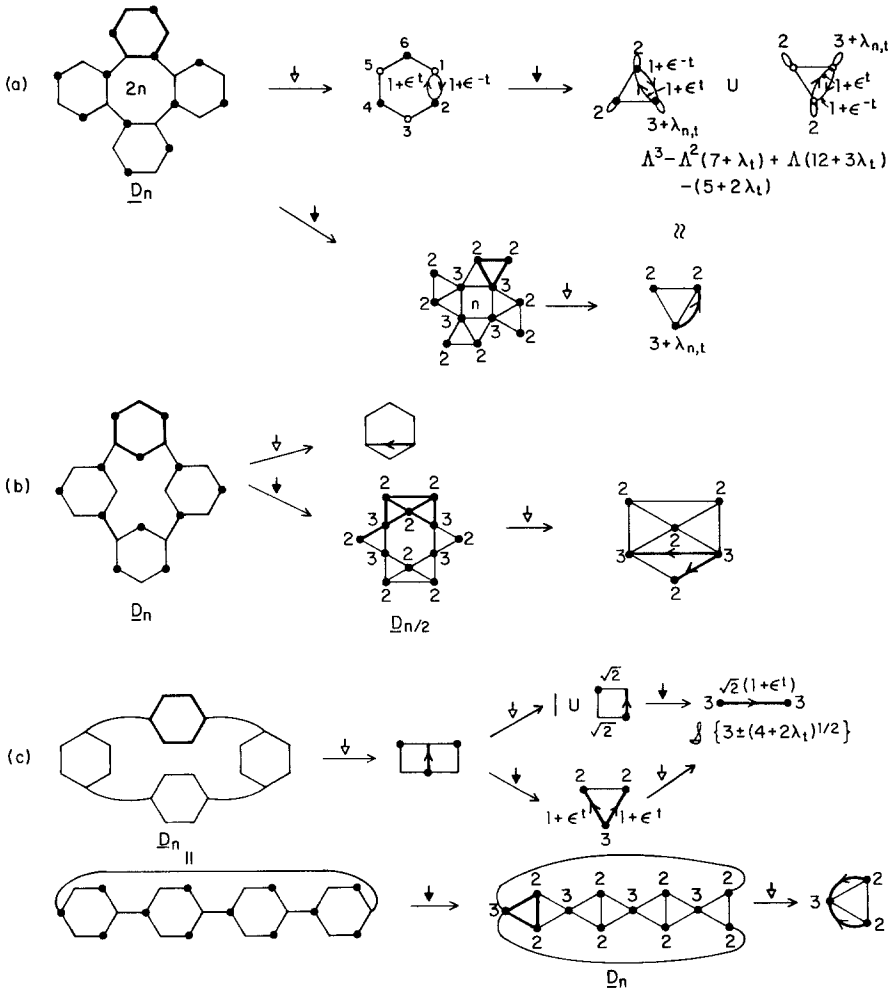
Fig. 4. Sequential automorphism–bipartite reduction of the ortho (a), meta (b), and para (c) cyclopolyphenylene graphs

Z_n reduction of the BRN. (The meta family is peculiar in that odd members are nonbipartite, and the Z_n ARN is also nonbipartite.) Sixth order matrices are predicted by group theory for degenerate IR's and bipartite reduction effectively lowers this order to three. The high symmetry of the para system enables a closed expression for squared eigenvalues.

Table 1 offers a selection of typical cyclopolymers suggested by Hückel molecular orbital applications [16, 17]. Their monomeric networks are reduced to the greatest possible extent for arbitrary IR's. As usual, the $t = 0$ case admits extraordinary reduction. The cyclacenes (a) are cyclic analogs of the common acene graphs. [4] Antisymmetric Z_2 reduction of a $[2n + 2]$cyclacene yields an $[n]$acene, so these familes are cosubspectral. Care must be exercised in dealing with the larger-ring acene analogs (b) and graphs like (e), since despite appearances, their odd members are nonbipartite. Eigenvalues of the looped cycle (c) are given in closed form; we must recognize that n in this case and in (i) and (j) is the number of monomers and the total ring size is 2n. Bipartite reduction of simple circuits furnishes the relation $\lambda^2(C_{2n}) = \lambda(C_n) + 2$, so the expression stated in (c) is in conformity with that developed previously (Ref. 2, Appendix theorem 2). When $\omega' = 0$, (c) and (d) become Z_2 reduction networks of graphs (a) and (b), respectively.

The trivial eigenvalue formula for the radialenes in (g) may be contrasted with Cotton's lengthy discussion of this system [13]. The alternately methylenated ring in (i) is easily evaluated by observing that its BRN is an n-cycle of loop weight three. Radialenes are generalized by structure (k), which may be expressed by the corona operation $C_n \circ mK_1$. The reduction network is a centrally looped star $(K_{1,m})$ whose further reduction yields the given spectrum.

It should be borne in mind that the A_1 state networks of many π-hydrocarbon cyclomers are graphs of molecules which would otherwise be dismissed as without significance in the realm of π-electron theory. Previous studies and the present investigation demonstrate that, within the Hückel context, distinction between π and non-π systems is not as rigid or meaningful as has long been assumed. This is to say that spectra of graphs traditionally understood as being associated with saturated molecules may well find themselves as subspectral networks of recognized and accepted conjugated structures. This point is emphasized in Fig. 5, where π-graph (a) is correlated with the norbornene dimer (!), and the novel, recently synthesized Kekulene (b) [19] with tricyclo-[3.2.1.0^{2,4}]-octane. Relationships such as these could never be appreciated or even imagined within the confines of molecular orbital theory. Since the reduction graph in, for example, (b), is related in other ways to a variety of superstructures, we have again spectrally "socialized" the benzenoid precursor.

The characteristic polynomial of complex edge-weight dinetworks like that in (b) is evaluated in (b') by the directed form of the Harary–Sachs theorem,

$$\alpha_k = \sum_{\vec{N}_k} (-1)^{c(\vec{N}_k)} \prod_e \omega[e(\vec{N}_k)],$$

where c is the number of components in an order k circuit subnetwork [3]. Fig. 5b′ only summarizes the essentials of the calculation for $k = 7$.

3. Topics in Automorphism Reduction

3.1. Graphs with Invariant Vertices: Stars and Rotors

Based upon the development of Sect. 2, we proceed to consider in more detail problems associated with invariant vertices. The graphs of Table 2 all have one or more fixed vertices, but the principal purpose is to examine the effect of relatively small structural elaborations on the spectrum of a constant subgraph ("frame")

Table 1. Complete reduction of cyclopolymeric graphs
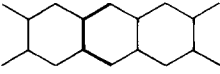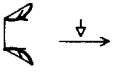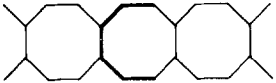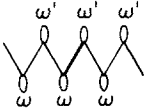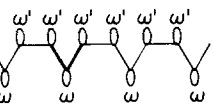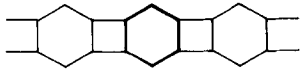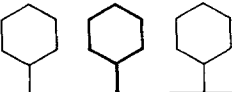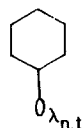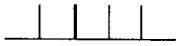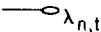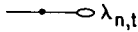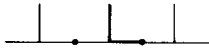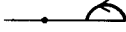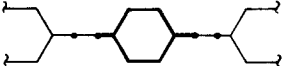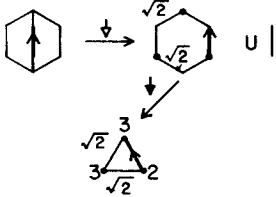
Table 1 (Cont.)

Cyclopolymer Motif	Z_n ARN

(g) Radialene

$$\longrightarrow\!\!\circ\ \lambda_{n,t}$$
$$\mathscr{L}:\left\{1/2\left[\lambda_t\pm(\lambda_t^2+4)^{1/2}\right]\right\}$$

(h) Pervinylannulene

$$\longrightarrow\!\!\bullet\!\!\longrightarrow\!\!\circ\ \lambda_{n,t}$$
$$\lambda^3-\lambda^2\lambda_t-2\lambda+\lambda_t$$

(i)

$$\mathscr{L}:\left\{\pm(3+\lambda_t)^{1/2}\right\}$$

(j)

$$\downarrow\!\!\downarrow$$
$$1\bullet\!\!\longrightarrow\!\!\bullet(3+\lambda_{n,t})$$
$$\Lambda^2-\Lambda(4+\lambda_t)+(2+\lambda_t)$$

(k)

$$\overset{m}{}$$
$$\lambda_{n,t}$$
$$\mathscr{L}:\left\{1/2\left[\lambda_t\pm(\lambda_t^2+4m)^{1/2}\right],0^{m-1}\right\}$$

(l)[18]

$$\Lambda^3-8\Lambda^2+16\Lambda-(5+2\lambda_t)$$

shown below. Higher homologs appearing in (l) and (m) are necessary for particular features not demonstrable by the odd Z_n system. Different monomer subgraphs for the parent and their cospectral ARN's are shown in (a)–(a'').

acepentylene

(a)

(b)

Kekulene

$$\phi(N) = \lambda^8 - 10\lambda^6 - \lambda^5 \lambda_t + 29\lambda^4 + \lambda^3 (3\lambda_t)$$
$$- 28\lambda^2 - \lambda(2\lambda_t) + (4 + \lambda_t^2)$$

(b') $\phi(N) = \Sigma a_k \lambda^{n-k}$

$a_7 = -2\lambda_t$:

(×2)

$2(-1)^2(\epsilon^t + \epsilon^{-t})$
‖
$2\lambda_t$

$2(-1)^2(\epsilon^t + \epsilon^{-t})$
‖
$2\lambda_t$

$3(-1)^3(\epsilon^t + \epsilon^{-t})$
‖
$-3\lambda_t$

$2(-1)^3(\epsilon^t + \epsilon^{-t})$
‖
$-2\lambda_t$

(×3)   (×2)

$(-1)(\epsilon^t + \epsilon^{-t})$
‖
$-\lambda_t$
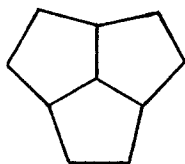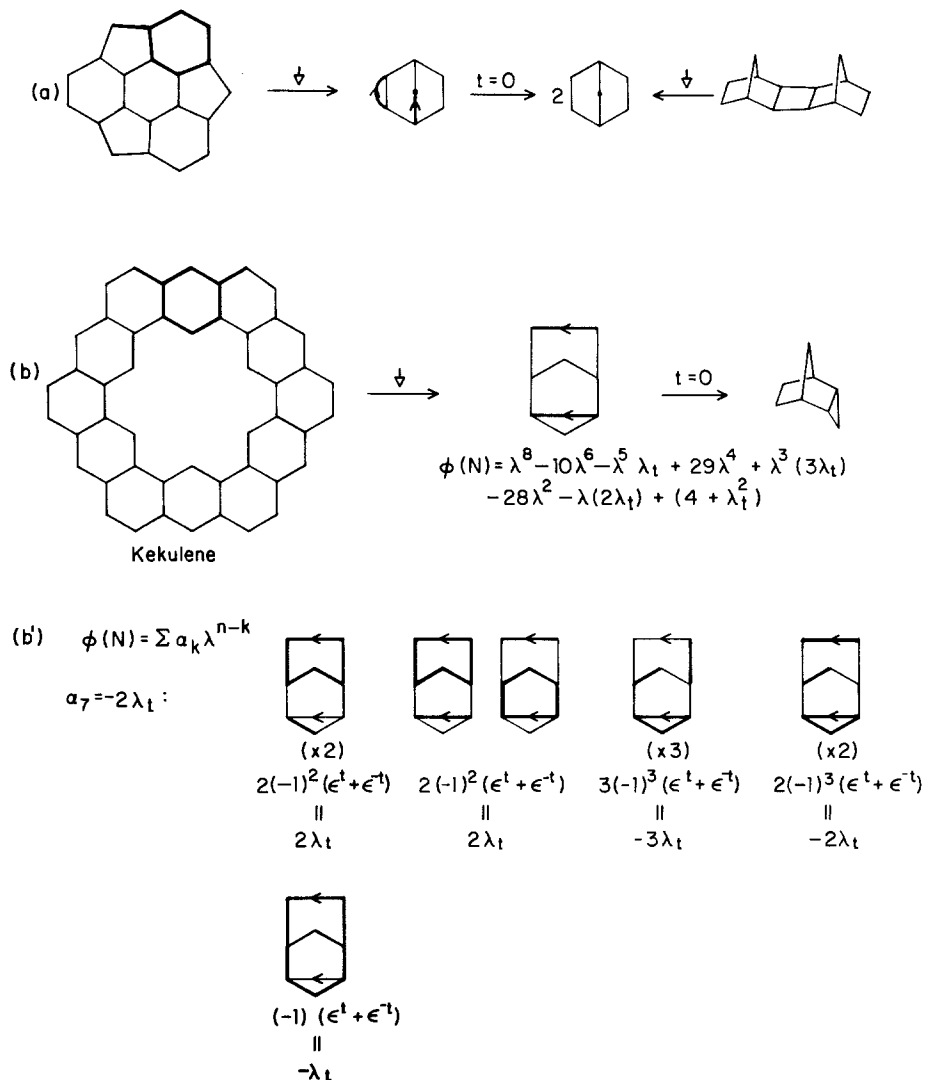
Fig. 5 (a, b) Spectral alliance of aromatic and nonaromatic graphs; (b') polynomial evaluation of dinetwork (b)

Reduction of each graph calls for identification of the spectrally significant structural elements discussed in the preceding section and supplementation of the frame ARN with the corresponding reduction component. *Any ARN can be written by inspection.* It is advantageous to separately specify both totally symmetric and non-totally symmetric constituents. From each of these we are able to deduce distinct cosubspectral relations, which may be either intrafamily or interfamily in nature. In many cases the reductions may be made to pertain to graphs homologous with those presented by simple adjustment of the $n^{1/2}$ edge weight; we must be judicious in these generalizations, however.

Table 2. Z_n automorphism reduction of graphs with a common subgraph
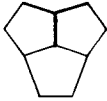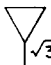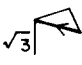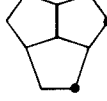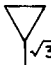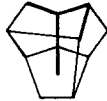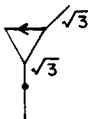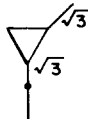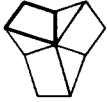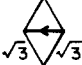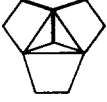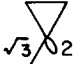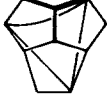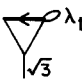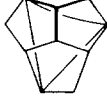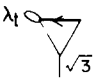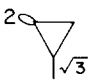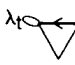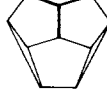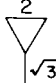
GRAPH	Z_n ARN	$A_1(t=0)$	$t \neq 0$
(a) $\mathscr{G}^\circ : D_3$ $3A_1 + A_2 + 3E$	$\sqrt{3}$	$\sqrt{3}$ $(\lambda^3 - \lambda^2 - 5\lambda + 3)(\lambda + 1)$	$\lambda^3 - 3\lambda - \lambda_t$
(a')	$\sqrt{3}$	"	"
(a")	$\sqrt{3}$	$\sqrt{3}$	$\lambda^3 - 3\lambda - \lambda t$
(b)	$\sqrt{3}$ $\sqrt{3}$	$\sqrt{3}$ $\sqrt{3}$	
(c)	$\sqrt{3}$ $\sqrt{3}$	$\sqrt{3}$ $\sqrt{3}$	"
(d)	$\sqrt{3}$ λ_t	$\sqrt{3}$ 2	λ_t $\lambda^3 - \lambda^2 \lambda_t - 3\lambda - 2$
(e)	λ_t $\sqrt{3}$	2 $\sqrt{3}$	λ_t $\lambda^3 - \lambda^2 \lambda_t - 3\lambda - 2$
(e')	λ_t $\sqrt{3}$	2 $\sqrt{3}$	λ_t $\lambda^3 - \lambda^2 \lambda_t - 3\lambda - 2$
(f)	$\sqrt{3}$	2 $\sqrt{3}$	$\lambda^3 - 3\lambda - (2 + \lambda_t)$

Table 2 (Cont.)

GRAPH	Z_n ARN	$A_1(t=0)$	$t \neq 0$
(g)	λt $\sqrt{3}$	2 $\sqrt{3}$ $\mathscr{I}_{n=3}\{3,1,-2^2\}$	λt $\lambda^3 - \lambda(2+\lambda_t^2) - 2\lambda_t$ $\mathscr{I}_{n=3}\{1^2,-2\}$
(h)	$\sqrt{3}$	2 $\sqrt{3}$	
(i)	$\sqrt{3}$	2 $\sqrt{3}$	$\lambda^3 - \lambda(4+\lambda_t) - (\lambda_t + \lambda_{2t})$
(j)	λ_t λ_t $\sqrt{3}$	2 2 $\sqrt{3}$	λ_t λ_t $\lambda^3 - \lambda^2(2\lambda_t) + \lambda(\lambda_t^2 - 3) + (\lambda_t - 2)$
(k)	$\sqrt{3}$	2 2 2 $\sqrt{3}$	$\lambda^3 - 3\lambda(2+\lambda_t) - (2+\lambda_t)^2$
(l)	2 $(-1)^t$	2	$(-1)^t$
(m)	$\sqrt{6}$ $(-1)^t$	2 $\sqrt{6}$	$(-1)^t$ $\lambda^2 - \lambda(-1)^t - (2+\lambda_t)$
(n)	$(\approx)$ $(-1)^t$ $\sqrt{6}$	$\sqrt{6}$	$(-1)^t$

A few remarks on specific Table 2 graphs are appropriate. Z_3 reduction of the parent graph (a) may be compared with Streitwieser's exposition [20] of D_3-adapted basis functions. In (b) both motif edges joining third order orbits to invariant vertices receive a $3^{1/2}$ weight. The $\lambda_{n,t}$ loops in (d) and (e) are associated with C_3 subgraphs. The graph (g) is a Z_3 conformer of the Petersen graph, to be discussed again later. The original ARN complex edges are supplemented by an oppositely directed, conjugately weighted pair. This is mandated by the presence of an edge joining the indicated subgraph to its clockwise neighbor at $2\pi/3$. The resultant is a symmetric edge of weight $\lambda_{3,t}$. Graphs (l)–(n) are required to probe the effect of intraorbit edges between v_q^i and $v_{q+n/2}^i$. Matrix element calculation occasions a network loop of weight $(-1)^t$.

The star graph $K_{1,n} = K_1 + \bar{K}_n$ and its uniform subdivisions $K_{1,n}^{(s)}$ are common constituents of larger graphs. Their wreath automorphism groups $E \times S_n[E_m](m = s + 1)$ are isomorphic to symmetric groups on n elements [10, 11].

$n = 6$

$K_{1,6}^{(0)}$ $K_{1,6}^{(1)}$ $K_{1,6}^{(2)}$ (x n-1)

m=1   m=2   m=3 $\mathscr{D}=A_1$ $\mathscr{D} \neq A_1$
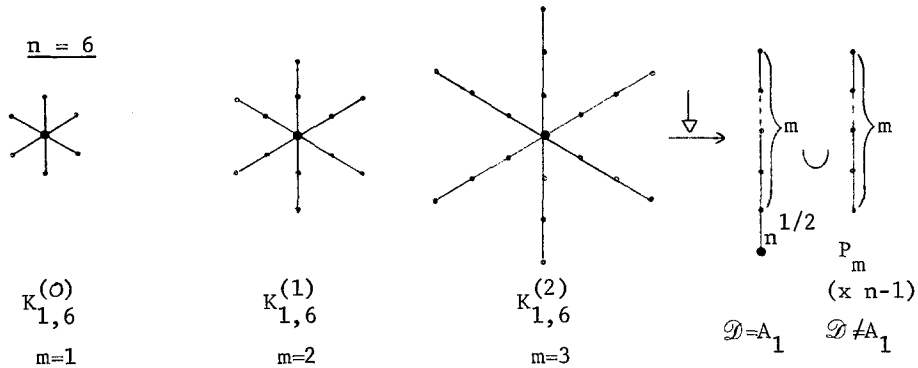
Only the S_n irreducible representations $[n]$ and $[n-1, 1]$ of dimension 1 and $n-1$, respectively, occur in the standard representation: $\mathscr{D}^0 = (m+1)\,[n] + m[n-1, 1]$. The P_m graph eigenvalues have multiplicity $n-1$ in the $K_{1,n}^{(s)}$ spectrum. As discussed elsewhere, exact solution of the A_1 network is possible only for the trivial cases $n = 1$ or 2; the general characteristic polynomial is $\phi(P_{m+1}) + (1-n)\phi(P_{m-1})$. The spectrum of the star is $\{\pm n^{1/2}, 0^{n-1}\}$ [15, 21]. Bipartite reduction is used to advantage in lowering the degree of algebraic expressions. Thus, for $s = 1$ we find $\mathscr{S}^2[K_{1,n}^{(1)}] = \{\mathscr{S}(K_n) + 2, 0\}$. Spectra of graphs of the general formula below are also available on this basis.
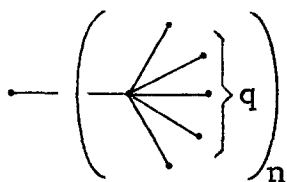
Compound star-like graphs such as the one shown below are evaluated by initially regarding one subgraph as fixed. Table 3 features a selection of structures containing invariant subgraphs and star-like subconfigurations. The $t \neq 0$
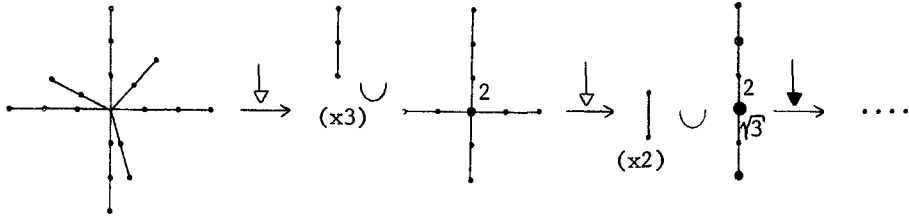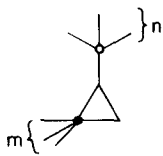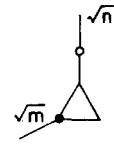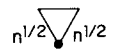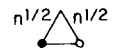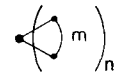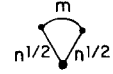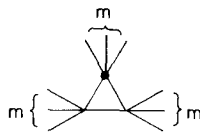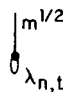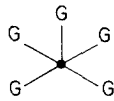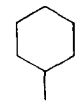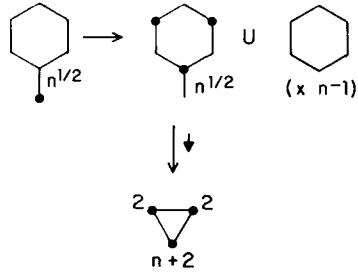

Table 3. Reduction of star subgraph systems

	GRAPH	ARN
(a)		
(b)		
(c)		
(d)		
(e)		
(f)		

Table 3 (Cont.)

GRAPH	ARN

(g)

(h)

$E \times S_n [S_2]$

$n^{1/2} \nabla n^{1/2}$ U |

$\mathcal{I} : \left\{ \tfrac{1}{2} \left[1 \pm (1 + 8n)^{1/2} \right] ; 1 \right\}$ $(\times n-1)$

(i)

$S_2 \times S_n$

$n^{1/2} \triangle n^{1/2}$ U $\cdot$ $(\times n-1)$

(j)

$\overset{m}{n^{1/2} \vee n^{1/2}}$

(k)

$\left| \, m^{1/2} \right.$

$\lambda_{n,t}$

(l)

$G \xrightarrow{n^{1/2}} \bullet \longrightarrow G$

$(t \neq 0)$

$G =$

$\longrightarrow$ U $(\times n-1)$

$\overset{2 \quad 2}{\underset{n+2}{\triangle}}$

$\mathcal{I} : \left\{ 1/2 \left[(n+5) \pm (n^2 - 2n + 9)^{1/2} \right] ; 1 \right\}$

$|V| = n = u + v + 2$

$n = x + y + 3$

$$u^{1/2} \quad v^{1/2} \quad U \quad \bullet \quad x(u+v-2)$$

$$x^{1/2} \quad y^{1/2} \quad U \quad \bullet \quad x(x+y-2)$$

$$u \quad \overset{u^{1/2}}{\bullet\!\!-\!\!\bullet} \quad v+1$$

$$\lambda^2 - \lambda(u+v+1) + \underline{uv}$$

$$x+1 \,\bullet\!\!-\!\!-\!\!\bullet\, y+1 \quad U \quad \bullet$$

$$\lambda^2 - \lambda(x+y+2) + \underline{(xy+x+y)}$$

$$uv = xy + x + y$$

$$(n-v-2)v = (n-y-3)(y+1) + y \xrightarrow{\;y=v+1\;} 2n = 3v + 7$$

$$n = 5 + 3k$$

n	v	y = v + 1
8	3	4
11	5	6
14	7	8
:	:	:

$$n = 11$$
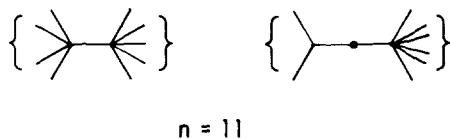
Fig. 6. Construction of two cospectral tree families

networks are obtained from A_1 by deleting the subgraph containing the prominent invariant vertex which is remote from the $n^{1/2}$ edge. In (a, b), (c, d), and (h, i), we have examples of A_1 cosubspectral graph pairs. Graph (f) consists (in molecular terms) of nested rotor subsystems, i.e. rotors of order m contained within rotors of order n. Families (h) and (j) were mentioned in the early report of Collatz and Sinogowitz [21]. The reduction of graphs of general structure (1) manifests the subgraph G. Triphenylmethyl is a celebrated representative of this

family; for $n = 3$ the formula given delivers its spectrum as $\{[\pm(4\pm3^{1/2})^{1/2},$ $\pm1, 0]_{t=0}[\pm1^4, \pm2^2]_{t=1,2}\}$.

Mowshowitz [22] first proved that there exist infinitely many pairs of cospectral trees. Fig. 6 employs cooperative automorphism and bipartite reduction to effect a simplified proof of his result. Equating coefficients of the two BRN polynomials and arbitrarily setting $y = v + 1$, integral solutions require that $n = 5 + 3k$, $k \geq 1$.

3.2. Families of One-Orbit Graphs

Graphs discussed to this point have been relatively simple, in the sense that connections between successive monomer subgraphs are few in number and of an easily deciphered character. Structures are now undertaken consisting of simple circuits which are crosslinked or chorded, i.e. vertices are joined in some repetitious fashion to others which are remote neighbors on the original cycle [23]. Multi-orbit graphs illustrating these somewhat more complex features are considered also. Spectral analysis finds that many families distinguished in graph theory have a common basis in the eigenvalues of circuits. Until now these relationships have been at best understood on an imprecise, intuitive level.

First we wish to deal with the prism $(Pr_n = C_n \times C_2)$ and antiprism $\tilde{Pr}_n$ families (Fig. 7). The prism spectrum derived from the reduction network is $\mathscr{S}(C_n) + \mathscr{S}(C_2)$, in agreement with the general graph product formula [14]. When n is even, a hamiltonian cycle can be displayed (a'), and automorphism reduction of this conformation takes a somewhat different, though spectrally equivalent, form. In algebraic manipulations the relations below are often useful. Bipartite reduction of even $[n]$prisms leads to antiprism-like networks of half the cycle

$$\bigcup_t \lambda_{n,2t} = \begin{cases} \mathscr{S}(C_{n/2}) & n \text{ even,} \\ \mathscr{S}(C_n) & n \text{ odd,} \end{cases} \qquad \mathscr{S}^2(C_n) = \mathscr{S}(C_{n/2}) + 2$$

order. This network spectrum is the square of the corresponding prism spectrum.

Several expressions are derived for the $[n]$antiprism (b), depending on the conformation being entertained. The last formula from the single orbit representation was derived by Rutherford [24] using matrix algebraic methods. The smallest antiprism is the octahedron, $K_{2,2,2}$, whose spectrum is calculated explicitly.

$K_{2,2,2}$

$$\mathscr{S}(C_3) = \{2, -1^2\} \qquad\qquad \mathscr{S}(C_6) = \{2, 1^2, -1^2, -2\}$$

$$\lambda_{n,t} \pm (\lambda_{n,t} + 2)^{1/2} \qquad\qquad \lambda_{m,t} + \lambda_{m/2,t}$$

$$n = 3 \quad 2 \pm 4^{1/2} = 4, 0 \qquad\qquad m = 6 \quad 2 + 2 = 4$$

$$-1 \pm 1^{1/2} = -2^2, 0^2 \qquad\qquad\qquad 1 + (-1) = 0^2$$
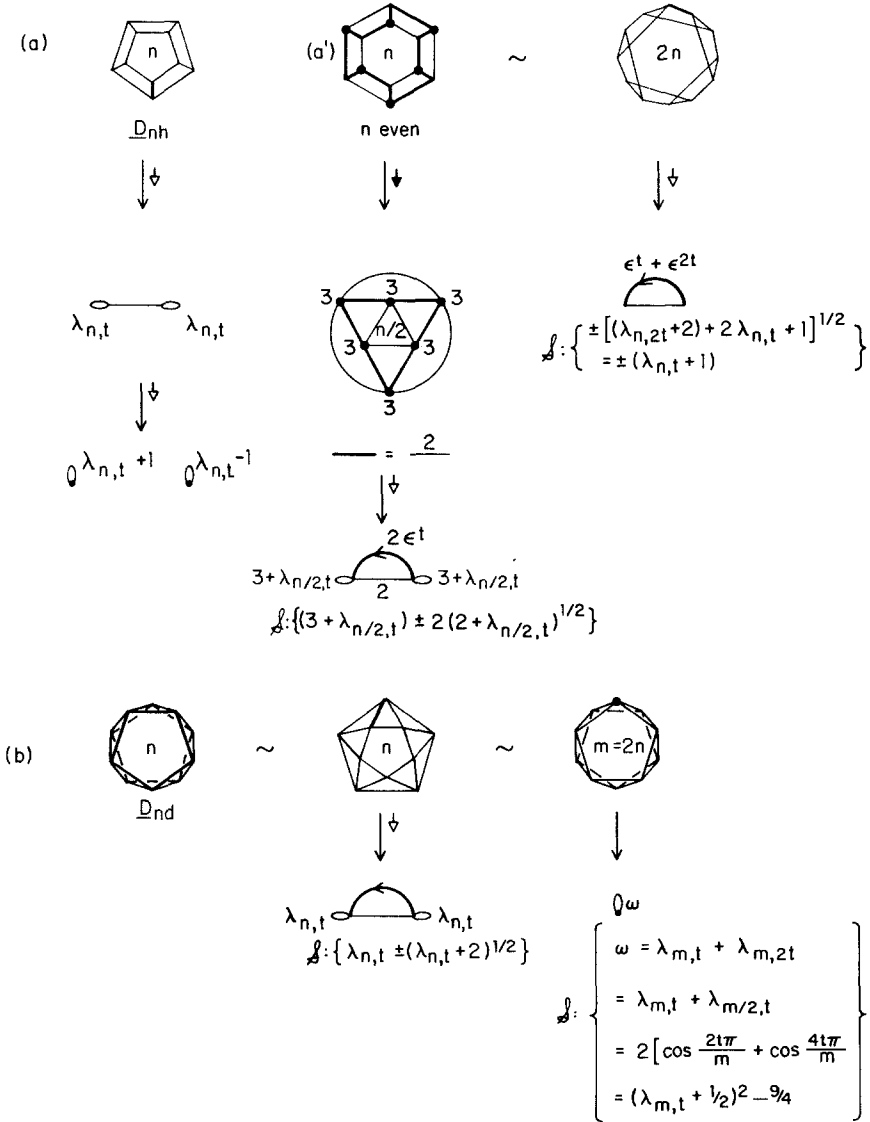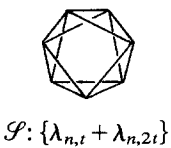
$$-1 + (-1) = -2^2$$

$$-2 + 2 = 0$$

Fig. 7. Reduction of prisms and antiprisms

Interestingly, the antiprism analysis is quite independent of the two C_n subgraphs contained within $C_{m=2n}$, i.e. the spectral expression pertains as well to odd peripheral cycles bearing $v_i v_{i+2}$ crosslinking edges.

$\mathscr{S}: \{\lambda_{n,t} + \lambda_{n,2t}\}$

The reduction network makes evident that only the localized nature of the crosslinking edges is relevant to the graph spectrum. K_5 (not shown) is the first member of the odd series.

K_6 $(-\tau)$ $\overset{2\ \ 3}{\underset{(2)}{\overbrace{\qquad}}}$ $(-\tau)$ $\lambda_{5,t} + \lambda_{5,2t} = 2\cos 2t\pi/5 + 2\cos 4t\pi/5$

$(\tau-1)$ $\overset{1\ \ 4}{\underset{}{}}$ $(\tau-1)$ $t = 0$ $2(2\cos 0) = 4$

C_5 $t \neq 0$ $(\tau-1) + (-\tau) = (-\tau) + (\tau-1) = -1$

Special cases arise whenever there is deviation from an established structural pattern. For $v_i v_{i+2}$ edges such a singularity occurs only at the trivial $m = 4$ cycle.

These considerations extend easily to linkages of more remote vertices, illustrated in Fig. 8. The reader may agree that direct spectral computation of these fairly complex structures or study of their adjacency matrix properties would suffer severely by comparison with network analysis. Of course we now know that it is the symmetry of the graph rather than its structural intricacy which decides the order and difficulty of the spectral problem. Fig. 8 portends several topics for closer inquiry. Thus, Möbius ladder graphs appear as members of the various series, and these are now isolated as a distinct class. See Fig. 9. Even ring ladders consist of $[n]$circuits and $n/2$ edges $v_i v_{i+n/2}$, while odd ladders contain the n edges $v_i v_{i+(n-1)/2}$.

The essential structural features of both subfamilies were focused on in Sect. 2, and the present results are identical with those given by Schwenk [14]. Bipartite reduction of even M_{4q+2} Möbius ladders induces odd M_{2q+1} Möbius ladder-like networks whose spectra are determined in a similar fashion.
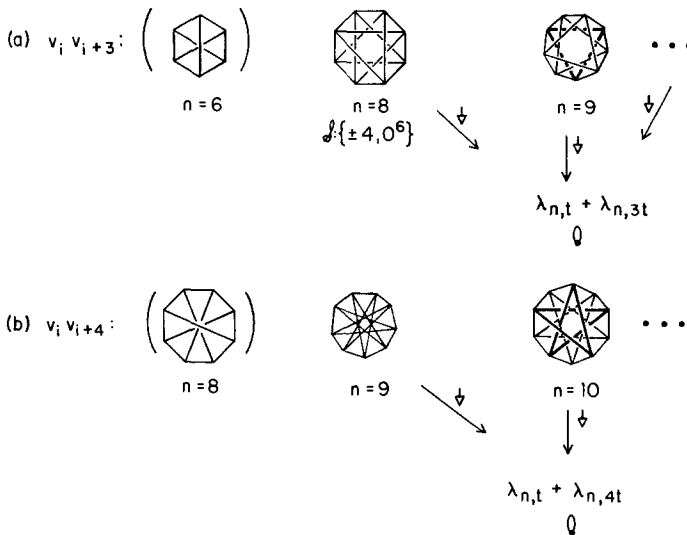

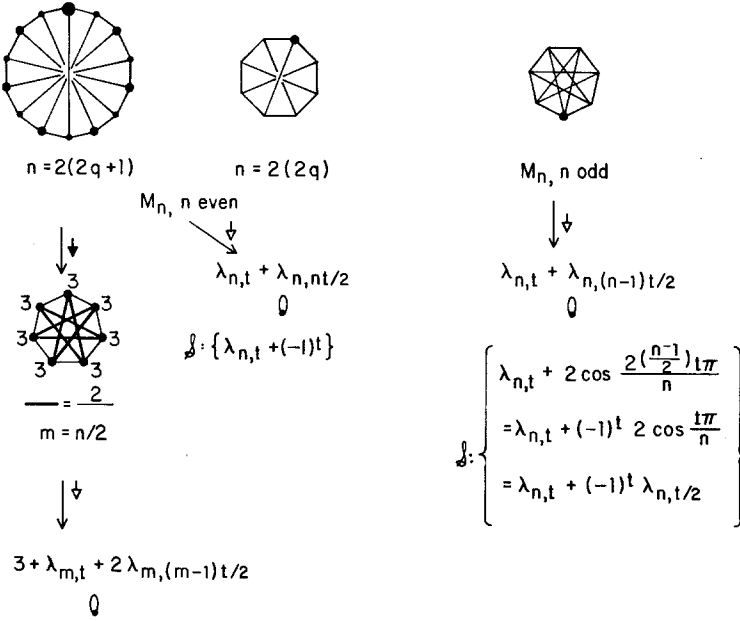**Fig. 8.** Z_n Reduction of crosslinked circuits

Fig. 9. Automorphism and bipartite reduction of Möbius ladders

The complete graphs K_n, wherein all vertices are nearest neighbors, are the next family to be determined (Fig. 10). The representation reduction under S_n is simply $\mathscr{D}^0 = [n] + [n-1, 1]$. Calculation of the matrix element proceeds as follows:

$$\lambda = \langle u^{(t)} | \hat{A} | u^{(t)} \rangle = n^{-1} \langle \sum \epsilon^{kt} v_k | \hat{A} | \sum \epsilon^{kt} v_k \rangle$$

$$= n^{-1} \langle \sum \epsilon^{kt} v_k | \sum \epsilon^{kt} (\sum_{j \neq k} v_j) \rangle$$

$$= n^{-1} \langle \sum \epsilon^{kt} v_k | \sum \epsilon^{kt} \sum_i v_{k \pm i} \rangle$$

$$= n^{-1} \langle \sum \epsilon^{kt} v_k | \sum \epsilon^{kt} \sum_{i=1} (\epsilon^{it} + \epsilon^{-it}) v_k \rangle$$

$$\vdots$$

$$= \lambda_{n,t} + \lambda_{n,2t} + \lambda_{n,3t} + \cdots + \begin{matrix} \lambda_{n,(n-2)t/2} + (-1)^t & n \text{ even} \\ \lambda_{n,(n-1)t/2} & n \text{ odd.} \end{matrix}$$

The final result could have been set down directly. When $t = 0$ the eigenvalue is $n - 1 = 2(n-2)/2 + 1 = 2(n-1)/2$. For the remaining roots we employ the identity [25] $\sum_{k=a}^{b} \cos 2kx = \cos (a+b)x \cdot \sin (-a+b+1)x / \sin x$ with $x = t\pi/n$. Some
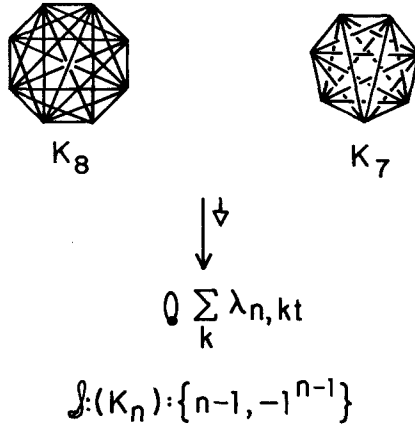
K_8 K_7

$$\downarrow \phi$$

$$0 \ \sum_k \lambda_{n,kt}$$

$$\mathscr{S}:(K_n):\{n-1,-1^{n-1}\}$$

Fig. 10. Reduction of complete graphs

trigonometric manipulation yields the well-known value (-1) for all

n even, t odd $\qquad \lambda = 0 + (-1) = -1$

n even, t even $\qquad \lambda = -2 + (+1) = -1$

n odd $\qquad\qquad \lambda = -1$

n and $t > 0$ [14, 15].

The complete bigraphs [14, 15] $K_{n,n}$ of Fig. 11 are drawn with a peripheral $m = 2n$ cycle having each vertex of one color class adjacent to the n vertices of the other located at $\pm 2\pi(2q+1)/m$. The spectrum is directly found to be

$$\mathscr{S}(K_{n,n}): \lambda_{m,t} + \lambda_{m,3t} + \cdots + \begin{matrix} \lambda_{m,(n-1)t} & n \text{ even,} \\ \lambda_{m,(n-2)t} + (-1)^t & n \text{ odd.} \end{matrix}$$

$K_{n,n}$: $K_{3,3}$ $K_{4,4}$ $K_{6,6}$ $K_{7,7}$

$(m = 2n)$ (Repeat Unit)

$$\sum_{k \text{ odd}} \lambda_{m,kt}$$

$$0$$

$$(m = 2n)$$

$$\dfrac{}{K_n(n) \cdot (n-1) \, K_n} \ , = \dfrac{n}{}$$
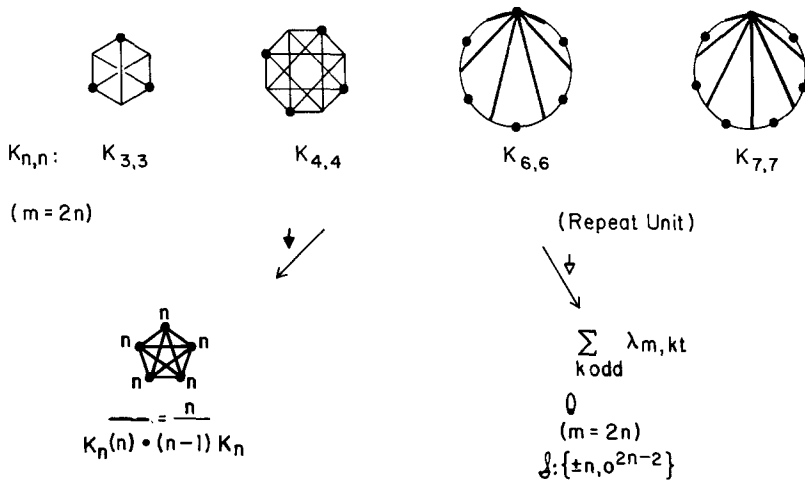
$$\mathscr{S}:\{\pm n, 0^{2n-2}\}$$

Fig. 11. Reduction of complete bigraphs, $K_{n,n}$

When $t = 0$, n the eigenvalues are respectively $2(n/2) = 2(n-1)/2 + 1 = n$ and $-2(n/2) = -2(n-1)/2 - 1 = -n$. Presumably, cosine summation with an odd argument yields the complementary zero eigenvalues. Bipartite reduction of $K_{n,n}$ creates the interesting complete network $K_n(n)$ with both loop and link edges of weight n.

Graphs (c)–(h) of Fig. 12 feature exterior and interior circuits which are mutually out of phase, i.e. they are star polygonal isomers of the corresponding [n]prisms. In (a) and (b) we demonstrate that the spectrum of an isolated circuit is invariant under conformational reorientation: modulo n, the same cosine arguments are encountered as t runs its course, though the order will vary. When two or more terms $\lambda_{n,t} + \lambda_{n,qt}$ are combined, however, the resultant is distinctive for each q. The cubic Petersen graph [26] was displayed in Table 2(g) with a threefold rotational axis (i.e. permutation cycles of length three); it is more economically treated in Fig. 12(c) in the higher order D_5 conformation. The principle of focusing on the maximal order subgroup, or more exactly, on an axial subgroup possessing a
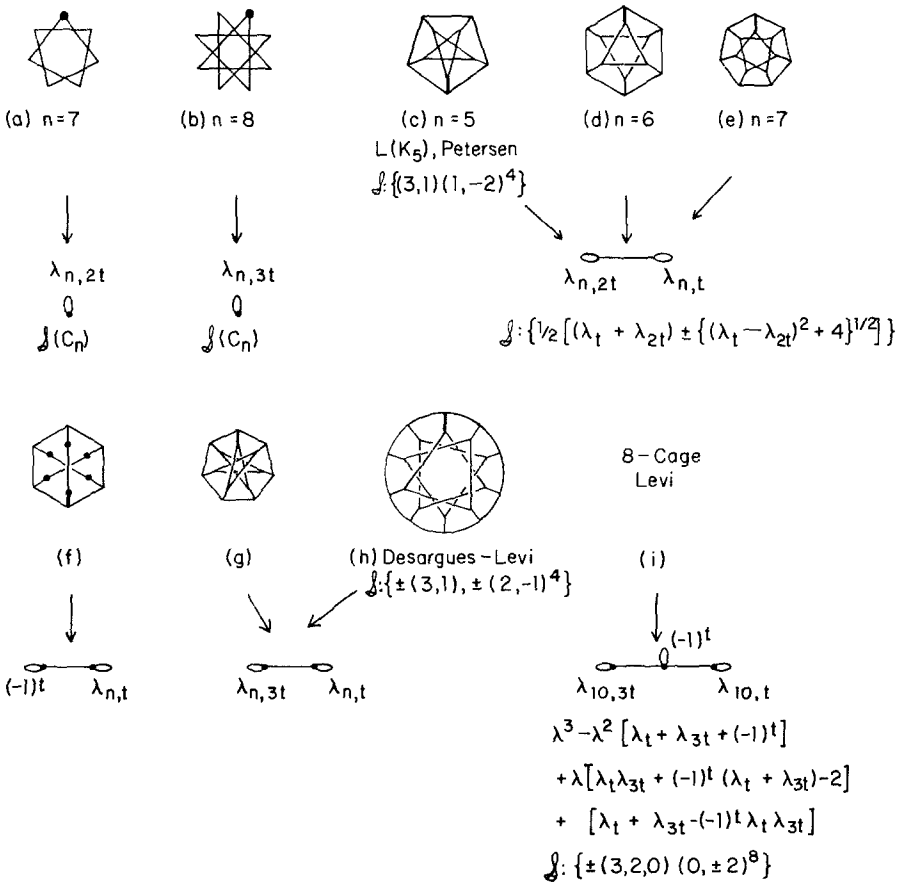

Fig. 12. Interpenetrating circuits

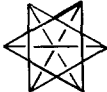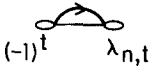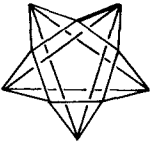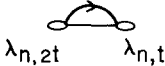**Table 4.** Structural effects and reduction
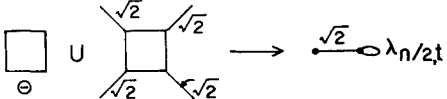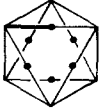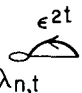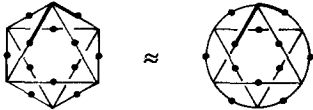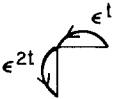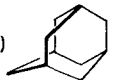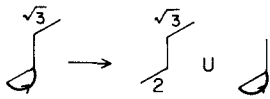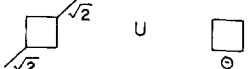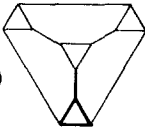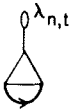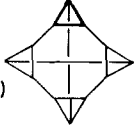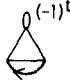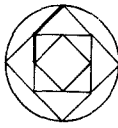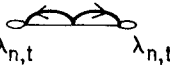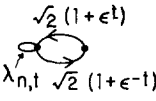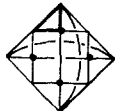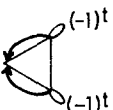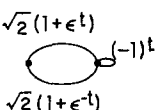
GRAPH	ARN

(a)

$(-1)^t \quad \lambda_{n,t}$

(b)

$\lambda_{n,2t} \qquad \lambda_{n,t}$

(c)

$\underline{D}_2 < \underline{D}_n$

$$\square \ominus \quad U \quad \boxed{}^{\sqrt{2}\ \sqrt{2}}_{\sqrt{2}\ \sqrt{2}} \longrightarrow \quad \bullet\!-\!\circ^{\sqrt{2}} \lambda_{n/2,t}$$

(d)

ϵ^{2t}

$\lambda_{n,t}$

$\jmath : \left\{ \tfrac{1}{2} \left[\lambda_t \pm (\lambda_t^2 + 4\lambda_{2t} + 8)^{1/2} \right] \right\}$

(e)

 $\approx$

ϵ^t

ϵ^{2t}

$(\lambda)(\lambda^2 - 4 - \lambda_t - \lambda_{2t})$

(f)

$\mathscr{O}^{\circ}(\underline{T}_d) = 2A_1 + E + 2F_2$

$\gtrless$

$\sqrt{3} \qquad \sqrt{3}$

$\longrightarrow \quad \cdot_2 \quad U$

$\jmath : \{ \pm 6^{1/2}, \pm 2^{1/2} \} \quad \jmath_{n=4} : \{ (0, \pm 2^{1/2})^2 \}$

(f')

$\underline{D}_2 < \underline{T}_d$

$\boxed{}^{\sqrt{2}}_{\sqrt{2}} \quad U \quad \square \ominus$

$\{ \pm 6^{1/2}, \pm 2^{1/2}, 0^2 \} \quad \jmath : \{ \pm 2^{1/2} (\times 2) \}$

Table 4 (Cont.)

GRAPH	ARN

(g)

$$\mathscr{D}^\circ(\underline{I}_d) = A_1 + E + F_1 + 2F_2$$

$\simeq$

(g')

$\underline{D}_4$

$\lambda_{n,t}$

$\mathscr{I}_{n=3} : \{ (3, \pm 2, -1)(\pm 2, 0, -1)^2 \}$

$(-1)^t$

$$\lambda^3 - \lambda^2(-1)^t - \lambda(4+\lambda_t) + (2+\lambda_t)((-1)^t - 1)$$

$$\mathscr{I}_{n=4} : \{ (3, 0, -2)(\pm 2, -1)^2(2, 0-1) \}$$

(h) Cuboctahedron ($\underline{O}_h$)

$\lambda_{n,t}$ $\xrightarrow{}$ $\sqrt{2}(1+\epsilon^t)$ $\lambda_{n,t}$ $\cup$ $0^{\lambda_{n,t}}$ $\lambda_{n,t}$ $\sqrt{2}(1+\epsilon^{-t})$

$$\mathscr{I}_{n=4} : \{ 4, 2^2, 0, -2^4 \} \quad \mathscr{J} : \{ \pm 2, 0^2 \}$$

(i)

$L(Q_3)$

$\lambda_{n,t}$ $\lambda_{n,t}$

$\| \mathscr{J}$

$\lambda_{n,t}$ $\lambda_{n,t}$ $\xrightarrow{\downarrow}$ $\sqrt{2}(1+\epsilon^t)$ $\cup$ $0^{\lambda_{n,t}}$ $\lambda_{n,t}$ $\sqrt{2}(1+\epsilon^{-t})$

$$n = 4 \quad \mathscr{J} : \{ 1/2 [\lambda_t \pm \{ \lambda_t^2 + 8(\lambda_t + 2) \}^{1/2}], \lambda_{n,t} \}$$

(i')

$(-1)^t$ $\xrightarrow{\downarrow}$ $\sqrt{2}(1+\epsilon^t)$ $(-1)^{t-1}$ $(-1)^{t+1}$ $\cup$ 0 $(-1)^t$ $\sqrt{2}(1+\epsilon^{-t})$

$$n = 4 \quad \mathscr{J} : \{ 1/2 [(-1)^t + 1] \pm [8\lambda_t + 18 + 2(-1)^t]^{1/2}, (-1)^t - 1 \}$$

minimal number of orbits, is a general one. Any graph analyzed in previous studies with respect to Z_2 can now be reconsidered with respect to possible higher order cyclic groups. The noteworthy spectral features of C_5 and its multiples in (c), (h), and (i) derive from properties of the classical number $\tau = 1/2(5^{1/2}+1) = 1.618033\ldots$. Thus, the general reduction formula for alternately linked interior vertices is easily evaluated to yield the Petersen spectrum. Its relation to the dodecahedron and Desargues–Levi eigenvalues was described in Part 2 of this series. The spectra of (f)–(h) involve the same quadratic formula as (c)–(e) with the parameter $\lambda_{n,qt}$. Compare the [7]prism with (e) and (g). Ten-fold cyclic symmetry in the cubic bigraphs (h) [27] and (i) and the τ recurrences favor extremely simple, highly degenerate, paired spectra. Depiction and discussion of the 5-unitransitive Levi graph may be found in Refs. 28 and 29. Cubic integral graphs are rationally and exhaustively constructed by Schwenk [26]. All structures exhibit very high symmetry, and it may now be possible to use this characteristic in independent proofs of his or similar graph theorems.

This Section concludes with a miscellaneous collection of graphs emphasizing remote monomer interaction and novel structural effects. Graph (c) of Table 4 is taken in a D_n conformation having $n/2$ invariant vertices. It is uncertain whether direct reduction modulo subgroups above Z_2 is possible in these systems. Graph
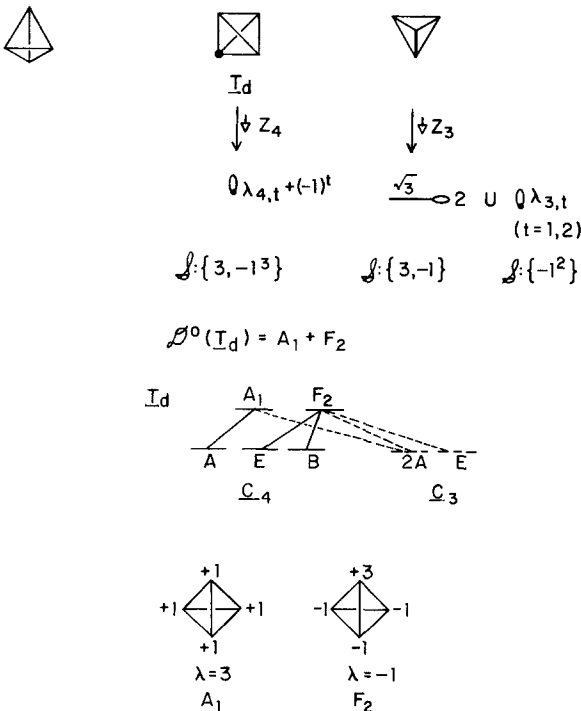

Fig. 13. Spectral reduction of the tetrahedron graph, representation correlation, and depiction of eigenvectors

(d) was discussed by Weimin [5], and (e) has a $K_{2,2,2}(4)$ bipartite reduction network (Fig. 18 of Ref. 1). The adamantane graph is reduced with respect to both Z_3 (f) and Z_2 (f'). Similarly, the truncated tetrahedron is reduced via Z_3 (g) and Z_4 (g'). The juxtaposition of eigenvalues associated with each subgroup irreducible representation should be noted. The cospectral pair (i), (i') [30] affirm that cospectral graphs need not be coreducible. Conceivably, other conformers or monomer choices would be coreducible, though there is no reason that they must be.

3.3. Platonic Eigenvalues; Polyhedral Spectra

Graphs of the five Platonic polyhedra are among the most interesting from the standpoint of symmetry. Figs. 13–17 treat Z_n automorphism reduction of the tetrahedron (K_4), cube $(Q_3 = C_4 \times C_2)$, octahedron $(K_{2,2,2})$, dodecahedron, and icosahedron, respectively. In addition to the reduction networks and spectra we show the irreducible representations occurring in these graphs, the representation correlation between $\mathscr{S}^0$ and Z_n, and diagrams (or equivalent specification) of typical eigenvectors associated with each eigenvalue. A complete spectral characterization of any graph would include these features. The procedure for forming eigenvectors is discussed by Collatz and Sinogowitz [21] and Streitwieser [20]. For the Platonic graphs, irreducible representations of the full group appear
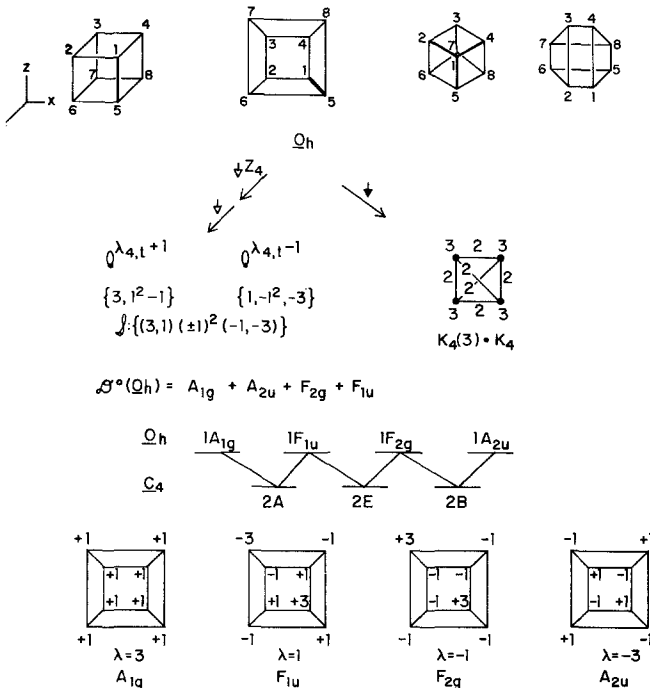

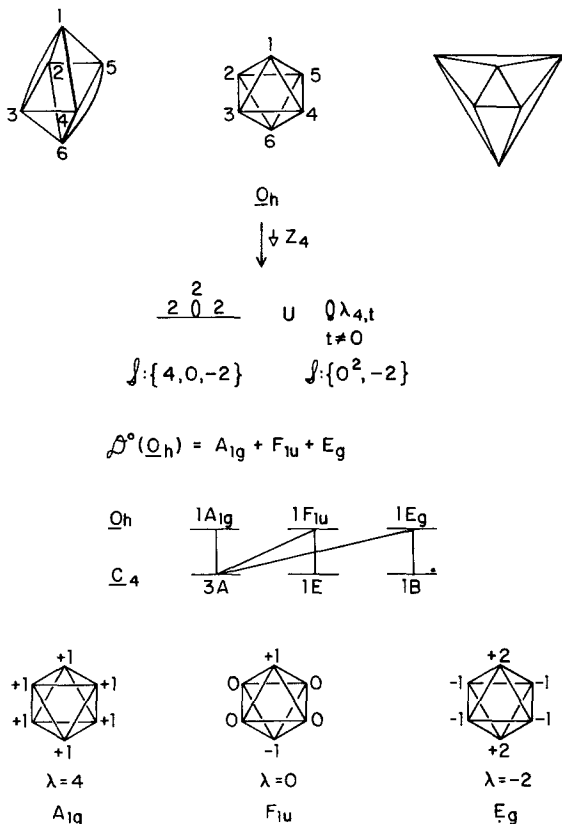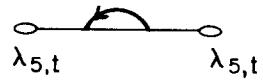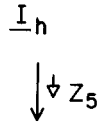**Fig. 14.** Cube spectral properties

Fig. 15. Octahedron spectral properties

at most once, and it is not particularly difficult to carry through the required manipulations. When a higher dimensional representation has a multiplicity of two or more, however, direct eigenvector construction can be extremely tedious (see, for example, Sect. 3.9 of Ref. 20). Observe that previously introduced notation clearly differentiates eigenvector components at a vertex from abbreviated representation of vertex loop weights in bipartite reduction networks.

The (non-Platonic) truncated icosahedron graph, whose Schlegel map appears in Fig. 18, corresponds to the hypothetical molecule C_{60}, a spheroidal, polyhedral oligomer of carbon and formally a trimer of bowl-shaped corannulene. Ordinarily, manual Hückel calculation of the electronic structure of such a large species would be considered prohibitive. Z_5 reduction affords a $|V| = 12$ network whose A_1 graph can be reduced to two quartic and two quadratic equations. Two twelfth order polynomials, both doubly degenerate, remain. Successive Z_2 reductions of the $|V| = 60$ graph provide equations of still lower degree, however. Z_2 irreducible components I and IV are easily disposed of by Z_3 reduction. The
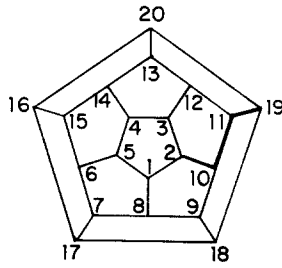
$$\lambda^4 - \lambda^3(2\lambda_t) + \lambda^2(\lambda_t^2 - \lambda_t - 4) + \lambda(2\lambda_t^2 + 6\lambda_t) - (\lambda_t^3 + 2\lambda_t^2 - 1)$$

$\lambda_{5,0} = 2 \qquad \mathscr{J}:\{\pm 5^{1/2}, 1, 3\}$

$\lambda_{5,1} = \lambda_{5,4} = \tau - 1 \qquad \mathscr{J}:\{5^{1/2}, 1, 0 - 2\}$

$\lambda_{5,2} = \lambda_{5,3} = -\tau \qquad \mathscr{J}:\{1, 0, -2, -5^{1/2}\}$

$\mathscr{J}^\circ(\underline{I}_h) = A_g + G_g + H_g + F_{1u} + F_{2u} + G_u$
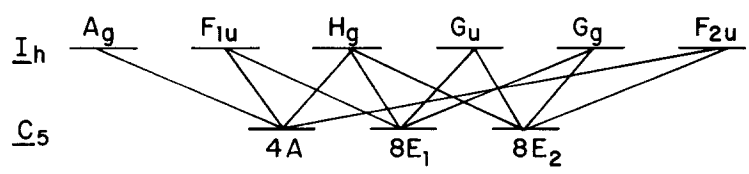
$A_g, \lambda = 3 \qquad \underline{u} = \displaystyle\sum_{i=1}^{20} i$

$F_{1u}, \lambda = 5^{1/2} \qquad \underline{u} = \big[3(1-20) + (2\tau-1)(2+5+8-13-16-19) + (3+4+6+7+9+10-11-12-14-15-17-18)\big]$

$H_g, \lambda = 1 \qquad \underline{u} = \big[3(1+20) + (2+5+8+13+16+19) - (3+4+6+7+9+10+11+12+14+15+17+18)\big]$

$G_u, \lambda = 0 \qquad \underline{u} = \big[2(1-20) - (3+4+6+7+9+10) + (11+12+14+15+17+18)\big]$

$G_g, \lambda = -2 \qquad \underline{u} = \big[6(1+20) - 4(2+5+8+13+16+19) + (3+4+6+7+9+10+11+12+14+15+17+18)\big]$

$F_{2u}, \lambda = -5^{1/2} \qquad \underline{u} = \big[3(1-20) - (2\tau-1)(2+5+8-13-16-19) + (3+4+6+7+9+10-11-12-14-15-17-18)\big]$

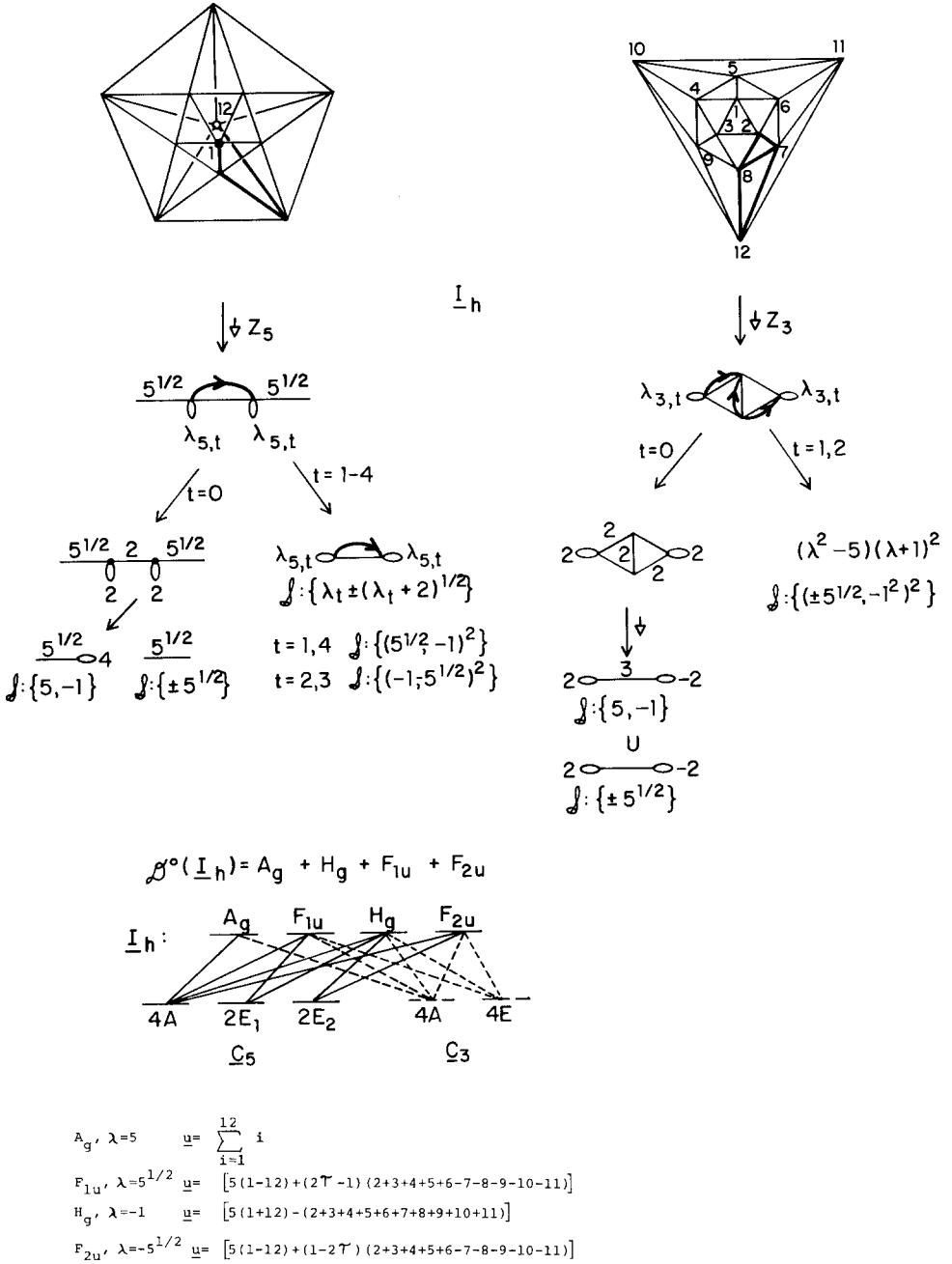**Fig. 16.** Dodecahedron spectral properties

Fig. 17. Icosahedron spectral properties
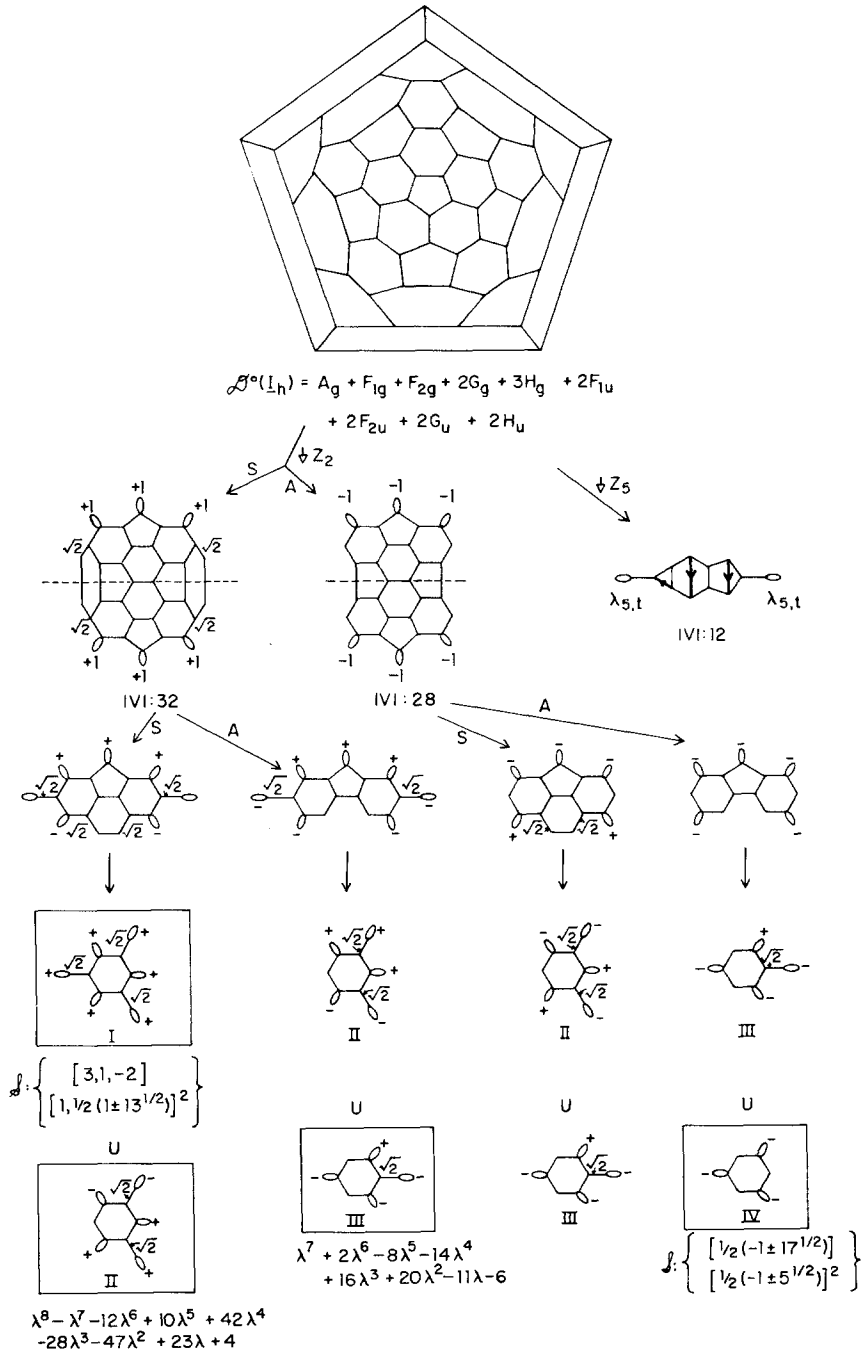
Fig. 18. Z_2 automorphism reduction of the truncated icosahedron, $|V| = 60$
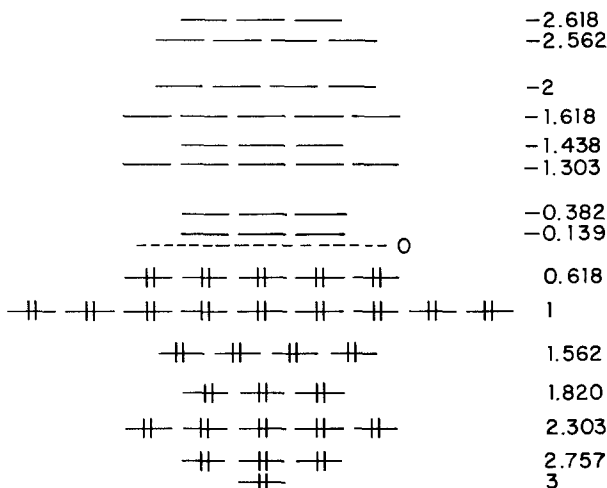
Fig. 19. Hückel orbital energies of truncated icosahedrane, C_{60}

spectra of the multiply occurring networks *II* and *III* are found by calculator to be

$$(II): \left\{ \begin{matrix} 2.757, & 1.820, & 1.562 = 1/2(-1+17^{1/2}), & 0.618, & -0.139 \\ & -1.438, & -1.618, & -2.561 = -1/2(1+17^{1/2}) & \end{matrix} \right\}$$

$$(III): \left\{ \begin{matrix} 2.303 = 1/2(1+13^{1/2}), & 1^2, & -0.382, & -1.303 = \\ 1/2(1-13^{1/2}), & -2, & -2.618 = -1/2(3+5^{1/2}) & \end{matrix} \right\}.$$

By assembling all these subspectra we arrive at the remarkable ELD of Fig. 19. The closed electronic shell and sizeable HOMO–LUMO gap are common characteristics of aromatic stability. More refined calculations and estimates of convex ring-distortion strain are warranted. Should such structures or their higher homologs ever be rationally synthesized or obtained by pyrolytic routes from carbon polymers, they would be the first manifestations of authentic, discrete, three-dimensional aromaticity. Stable cationic and anionic polyhedral C_n species might also be produced under appropriate conditions.

4. Conclusion

We have seen how graphical structures in their various conformations may be conceived as polymers of simple subgraphs and how this view facilitates eigenvalue computation. Spectra are decomposed into subsets corresponding to irreducible representations of cyclic groups. The t values of the subspectral networks serve as "quantum numbers" identifying eigenvalues with respect to a particular subgroup. Graphs of π-hydrocarbons are usually of such simple construction as to permit instant evaluation of the irreducible networks.

The principles of Z_n automorphism reduction of one-dimensional cyclopolymers extend easily to cyclic two-dimensional arrays, i.e., monomers embedded on a torus. The spectrum of a toroidally embedded quadratic lattice (with even

diameters) contains a planar quadratic lattice as a subspectrum, since antisymmetry planes cut out this fragment. The implication (later qualified) of Heilbronner's discussion [4] is that families of condensed benzenoid systems [31] derive analogously from toroidally embedded hexagonal cell precursors. In fact, only one of the two necessary types of antisymmetric reduction leads to loopfree graphs, and no relation is found between planar aromatic hydrocarbon spectra and toroidal-based cyclopolymer analogs.

Addendum

Since completion of this manuscript, three additional papers from the chemical literature devoted to characteristic equation factorization have come to our attention: B. J. McClelland, J. Chem. Soc., Faraday Trans. II **70**, 1453 (1974); R. B. King, Theoret. Chim. Acta (Berl.) **44**, 223 (1977); and S. S. D'Amato, Molec. Phys. **37**, 1363 (1979).

References

1. Davidson, R. A.: Genesis and synthesis of cospectral and paracospectral graphs. To be published.
2. Davidson, R. A.: Symmetry, spectra, and bigraph division. To be published.
3. Davidson, R. A.: On the symmetry and spectra of molecular graphs. To be published.
4. Heilbronner, E.: Helv. Chim. Acta **37**, 921 (1954).
5. Weimin, L.: Scientia Sinica **22**, 539 (1979)
6. Au-chin, T., Yuan-sun, K.: Scientia Sinica **19**, 207 (1976)
7. Au-chin, T., Yuan-sun, K.: Scientia Sinica **20**, 595 (1977)
8. Ledermann, W.: Introduction to group characters. New York: Cambridge Univ. Press. 1977
9. Jansen, L., Boon, M.: Theory of finite groups. Amsterdam: North Holland 1967
10. Hamermesh, M.: Group theory. Reading, Mass.: Addison-Wesley 1962
11. Coleman, A. J. in: Adv. in quantum chem. **4**, 83 (1968)
12. Serre, J., in: Molecular orbitals in chemistry, physics and biology, p. 133–149, Lowden, P., Pullman, B., Eds. New York; Academic Press 1964
13. Cotton, F. A.: Chemical applications of group theory. New York: Wiley Interscience 1963
14. Schwenk, A. J., in: Graphs and combinatorics p. 153–172, Bari, R., Harary, F., Eds. New York: Springer–Verlag 1974
15. Schwenk, A. J., Wilson, R. J., in: Selected topics in graph theory, p. 307–336 Beineke, L. W., Wilson, R. J., Eds. New York: Academic Press 1978
16. Streitwieser, Jr., A., Brauman, J. I.: Supplemental tables of molecular orbital calculations. New York: Pergamon Press 1965
17. Heilbronner, E., Straub, P. A.: Hückel molecular orbitals. New York: Springer–Verlag 1966
18. Bochvar, D. A., Stankevich, I. V.: J. Struct. Chem. **8**, 841 (1967)
19. Diederich, F., Staab, H. A.: Ang. Chem., Int. Ed. Engl. **17**, 372 (1978)
20. Streitwieser, Jr., A.: Molecular orbital theory for organic chemists New York: John Wiley 1961
21. Collatz, L., Sinogowitz, U.: Abh. Math. Sem. Univ. Hamburg **21**, 63 (1957)
22. Mowshowitz, A.: J. Combinatorial Theory **12B**, 177 (1972)
23. Elspas, B., Turner, J.: J. Combinatorial Theory **9**, 297 (1970)
24. Rutherford, D. E.: Royal Soc. Edinburgh **63A**, 232 (1950–51)
25. Polansky, O. E.: Monatsheft f. Chem. **91**, 916 (1960), Appendix I

26. Schwenk, A. J., in: Theory and applications of graphs, p. 516–533 Alavi, Y., Lick, D. R., Eds. New York: Springer–Verlag 1978
27. Randić, M.: Intern. J. Quantum Chem. **15**, 663 (1979)
28. Harary, F.: Graph Theory. Reading, Mass.: Addison–Wesley 1969
29. Tutte, W. T.: Connectivity in graphs. Toronto: Univ. of Toronto Press 1966
30. Godsil, C., Holton, D. A., McKay, B., in: Combinatorial mathematics V, p. 111 Little, C. H. C., Ed. New York: Springer–Verlag 1977
31. Rutherford, D. E.: Royal Soc. Edinburgh **A62**, 229 (1947)